
UNIVERSITE DE LAUSANNE – FACULTE DE BIOLOGIE ET DE MEDECINE

DMCP - CHUV

Laboratoire d'oncologie pédiatrique

Role of *ALK* gene and mutations in initiation and progression of neuroblastoma

THESE

préparée sous la direction du Docteur Nicole Gross
avec la collaboration du Docteur Annick Mühlethaler

et présentée à la Faculté de biologie et de médecine de
l'Université de Lausanne pour l'obtention du grade de

DOCTEUR EN MEDECINE

par

QZ
380
MON

BMTE 3749

Gisèle MONTAVON

Médecin diplômée de la Confédération Suisse

Originaire de Montavon (Jura)

Lausanne

2014

Bibliothèque Universitaire
de Médecine / BiUM
CHUV-BH08 - Bugnon 46
CH-1011 Lausanne

Imprimatur

Vu le rapport présenté par le jury d'examen, composé de

Directeur de thèse *Madame le Docteur Nicole Gross*
Co-Directeur de thèse
Expert *Madame le Professeur Monika Hegi*
Directrice de l'Ecole *Madame le Professeur Stephanie Clarke*
doctorale

la Commission MD de l'Ecole doctorale autorise l'impression de la thèse de

Madame Gisèle Montavon

intitulée

*Role of ALK gene and mutations in initiation and progression
of neuroblastoma*

Lausanne, le 18 février 2014

*pour Le Doyen
de la Faculté de Biologie et de Médecine*



*Madame le Professeur Stephanie Clarke
Directrice de l'Ecole doctorale*

Informations générales

Doctorante

Gisèle Montavon
Pérolles d'en Haut 9
1752 Villars-sur-Glâne
gi.montavon@gmail.com
079/300.07.39

Lieu de l'étude

Laboratoire d'oncologie pédiatrique
CHUV - DMCP
Rue du Bugnon 46
1011 Lausanne

Directrice de thèse

Dr Nicole Gross, Privat-Docent & MER
CHUV - DMCP
Rue du Bugnon 46
1011 Lausanne
nicole.gross@chuv.ch
021/314.17.46

Jury de thèse

- Dr Nicole Gross (directrice de thèse)
- Prof. Monika Hegi (experte)
- Prof. Stephanie Clark (directrice de l'Ecole
doctorale)

Responsable de thèse

Dr Annick Mühlethaler
CHUV - DMCP
Rue du Bugnon 46
1011 Lausanne
annick.muethaler@chuv.ch
021/314.36.15

Collaborateurs :

- Madame Katia Balmas Bourloud
CHUV - DMCP
Rue du Bugnon 46
1011 Lausanne
- Dr Jean-Marc Joseph et Dr Nicolas Jauquier
CHUV - DMCP
Rue du Bugnon 46
1011 Lausanne

Collaborations :

- Dr Isabelle Janoueix-Lerosey et Dr Olivier Delattre
Institut Curie
Rue d'Ulm 26
75005 Paris
- Prof. Lukas Sommer
Institute of Anatomy
Zurich University
Winterthurerstrasse 190
8057 Zürich

Table of contents

Résumé.....7

Abbreviations.....9

Introduction.....11

Aims of the project.....20

Materials and methods.....21

Results.....27

Discussion.....46

Conclusion and perspectives.....54

Acknowledgements.....56

References.....57

CURRICULUM VITAE.....61

Résumé

Introduction

Le neuroblastome (NB) est la tumeur maligne solide extra-crânienne la plus fréquente chez l'enfant. Sa présentation clinique est très hétérogène, allant d'une tumeur localisée à une atteinte métastatique sévère. Malgré des traitements agressifs, environ 55% des NB de hauts risques sont actuellement résistants aux thérapies. L'espoir réside dans le développement de traitements ciblant les mécanismes moléculaires responsables du développement et de la progression du NB. Le gène Anaplastic Lymphoma Kinase (ALK) codant pour un récepteur tyrosine kinase a été particulièrement étudié ces dernières années car il est muté, amplifié ou surexprimé dans une majorité des NBs. Le but de ce projet était d'investiguer le rôle de ALK-wt, ainsi que de ces deux plus fréquentes mutations, ALK-F1174L et ALK-R1245Q, dans l'oncogenèse du NB. Le NB étant originaire des cellules de la crête neurale, nous avons analysé le potentiel oncogénique de ces différentes formes de ALK dans des cellules progénitrices de la crête neurale (NCPC).

Méthode

Des NCPC de souris (JoMa1), possédant un c-MycER inductible pour leur maintien en culture *in vitro*, ont été transduites par un rétrovirus permettant l'expression stable de ALK-wt, ALK-F1174L et ALK-R1245Q. Des tests *in vitro* ont d'abord été effectués pour tester le système c-MycER, la stabilité de nos cellules transduites, leur phénotype, leur capacité de croissance et leur tumorigénicité. Les cellules transduites ont ensuite été injectées dans des souris immunosupprimées en sous-cutané, puis en orthotopique, c'est-à-dire dans leur glande surrénale, afin de mesurer leur tumorigénicité *in vivo*.

Résultats

La transduction et l'expression stable de ALK n'ont pas modifié le phénotype indifférencié des JoMa1, ni de manière significative la capacité de croissance des cellules *in vitro* en absence d'activation de c-MycER. Par contre, lorsque c-MycER est actif, les cellules porteuses des mutations F1174L et R1245Q ont montré une meilleure capacité de prolifération et de formation de colonies, par rapport aux JoMa1-ALK-wt et aux cellules contrôles en culture 3D dans de la méthylcellulose et dans un test de formation de neurosphères. *In vivo*, les souris injectées avec les cellules JoMa1-ALK-F1174L en sous-cutané ou dans la glande surrénale ont rapidement développé des tumeurs, suivies par le groupe JoMa1-ALK-R1245Q et le groupe JoMa1-ALK-wt, alors que les groupes de souris contrôles n'ont présenté aucune tumeur. En orthotopique, nous avons obtenu 5/6 tumeurs ALK-F1174L, 7/7 tumeurs ALK-R1245Q et 6/7 tumeurs ALK-wt. Les tumeurs sous-cutanées ne présentaient pas de différences morphologiques et histologiques entre les différents groupes et montraient une histologie compatible avec un NB. Les tumeurs orthotopiques restent encore à analyser.

Conclusion

Cette étude a permis de démontrer que les mutations activatrices F1174L et R1245Q ont des propriétés tumorigéniques *in vitro* dans des NCPC et *in vivo* tandis que la forme sauvage de ALK montre une capacité oncogénique uniquement *in vivo*. Bien que la caractérisation des tumeurs orthotopiques n'a pas encore été effectuée, l'analyse des tumeurs sous-cutanées nous suggère que l'expression de ALK-wt ou muté est suffisante pour induire la formation de NB à partir des cellules progénitrices de la crête neurale. Le gène ALK semble donc jouer un rôle important dans l'oncogénèse du NB, aussi bien par la présence de mutations activatrices que par sa fréquente surexpression.

Abbreviations

ALK-wt	Wild-type ALK
CEE	Chicken Embryo Extract
DMEM	Dubbecco's modified Eagle's medium
FCS	Foetal Calf Serum
FDA	Food and Drug Administration
GFP	Green fluorescent protein
INRG	International Neuroblastoma Risk Groupe
INSS	International Neuroblastoma Staging System
LAG	Left adrenal gland
MK	Midkine
NB	Neuroblastoma
NCPC	Neural crest progenitor cells
NCSC	Neural crest stem cells
NCSm	Neural crest sphere medium
PBS	Phosphate buffered saline
PCV	Pellet cells volume
PTN	Pleiotrophin
Rpm	Rotation per minute
RT	Room temperature
RTK	Receptor tyrosine kinase
SNS	Sympathetic nervous system
TBS	Tris-Buffered Saline

Introduction

Neuroblastoma

Neural crest cells are a transient population of neuroectodermal pluripotent cells in vertebrate embryo. During their anterior or posterior neural migration, they differentiate to give rise to various mature cell types as neurons, glial cells, melanocytes, chondrocytes, bone cells, myofibroblasts, adipocytes and endocrine cells [1, 2], as illustrated in Figure 1. Neuroblastoma (NB) is an embryonal tumor derived from neural crest progenitor cells (NCPC) [3] involved in the sympathetic nervous system development [4].

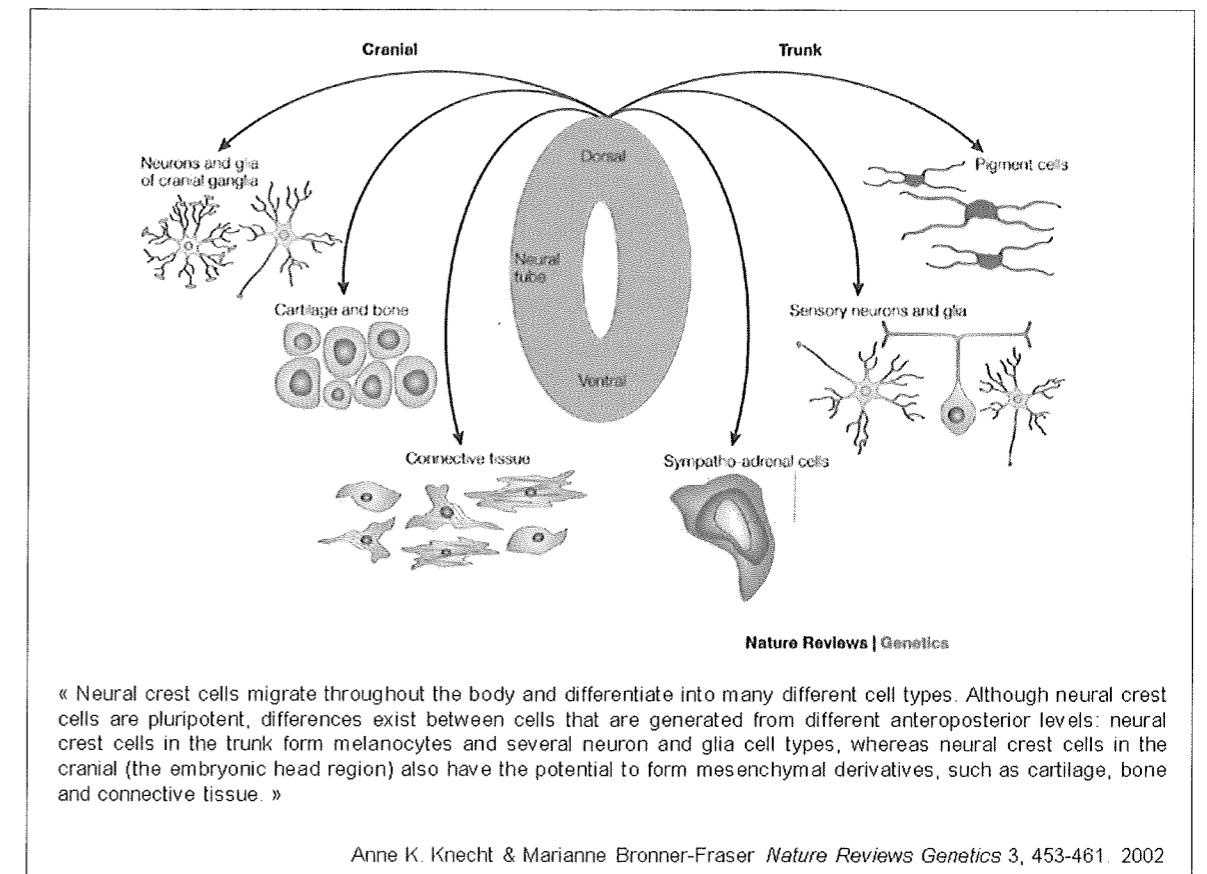


Figure 1: Neural crest cells migration and differentiation, from [5]

NB was first described in 1910 by Dr James Homer Wright [6] and nowadays its frequency is about 7% of cancers in children younger than 15 years [7], 30% of cancers in newborns [8], in addition to accounting for 15% of deaths in pediatric oncology [7]. Therefore, it is the most common and deadly extracranial solid tumor found in children, with a median age of 17 months at diagnosis [9].

NB develops in different anatomic sites of sympathetic nervous system: about 50% of NB in the adrenal medulla with the remaining portion distributed among cervical, thoracic, abdominal or pelvic sympathetic ganglia [10]. The heterogeneity of sites can be explained by the migration pattern of immature neuroblasts during fetal development of sympathetic nervous system.

Clinical presentations range from local tumors without symptom to severe metastatic disease, depending on tumor localization, volume and degree of invasion. Metastatic disease occurs by lymphatic or hematogenous tracts and can involve bone marrow, bone, lymph nodes, liver, intracranial and orbital sites, lung and central nervous system [11]. NB of 4S stage (“S” for “special”) is an exception with metastasis restricted to liver, bone marrow and skin [11]. Tumor and metastasis can compress digestive, respiratory, neurologic and urinary systems. Orbital metastasis can manifest with periorbital swelling and proptosis (“raccoon eyes”) and skin metastasis as blue subcutaneous nodules [12]. Catecholamines secretion can induce tachycardia and hypertension [12]. Two major paraneoplastic syndromes are associated with NB, which are secretion of vasoactive intestinal peptide (VIP) inducing intractable secretory diarrhea, and opsoclonus-myoclonus syndrome (rapid eye movements, ataxia and myoclonus) [7].

The diagnosis of NB is confirmed by histopathological analysis of tumor tissue or the presence of typical NB cells in bone marrow biopsy, combined with elevated catecholamines concentrations in urinalysis [7]. Metaiodobenzylguanidine (mIBG) scintigraphy is used to evaluate extent of disease, response to treatment and post-therapy evolution [13]. The stage at diagnosis was previously scored with the International Neuroblastoma Staging System [14], according to the extent of disease, as illustrated in Figure 2 and described in Table 1.

Stage	Definition
I	Localized tumor with complete gross excision, with or without microscopic residual disease; representative ipsilateral lymph nodes negative for tumor microscopically (nodes attached to and removed with the primary tumor may be positive).
IIA	Localized tumor with incomplete gross excision; representative ipsilateral nonadherent lymph nodes negative for tumor microscopically.
IIB	Localized tumor with or without complete gross excision, with ipsilateral nonadherent lymph nodes positive for tumor. Enlarged contralateral lymph nodes must be negative microscopically.
III	Unresectable unilateral tumor infiltrating across the midline, with or without regional lymph node involvement; or localized unilateral tumor with contralateral regional lymph node involvement; or midline tumor with bilateral extension by infiltration (unresectable) or by lymph node involvement.
IV	Any primary tumor with dissemination to distant lymph nodes, bone, bone marrow, liver, skin and/or other organs (except as defined for stage 4S).
IVS	Localized primary tumor (as defined for stage 1, 2A or 2B), with dissemination limited to skin, liver, and/or bone marrow (limited to infants < 1 year of age)

Table 1: International Neuroblastoma Staging System, from [14], previous classification.

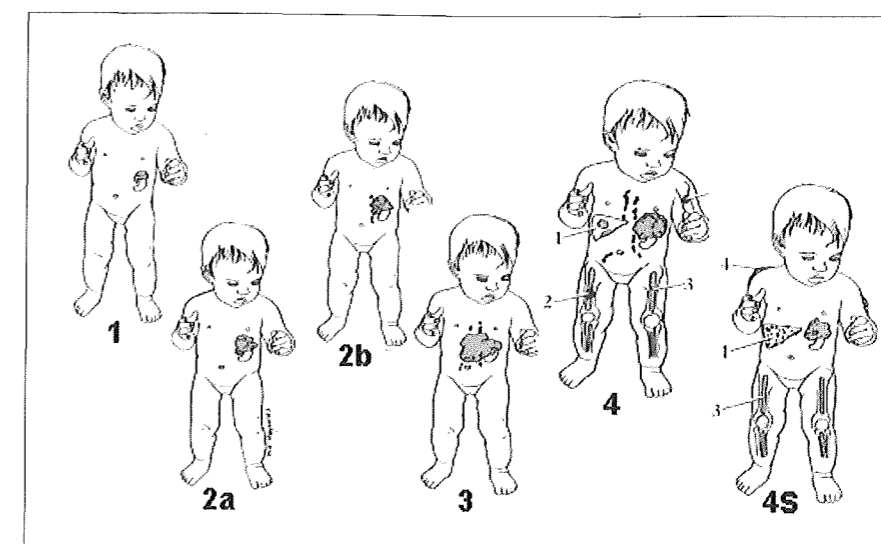


Figure 2: Illustration of International Neuroblastoma Staging System (INSS), from <http://www.nant.org/pix/inss.jpg>

The aetiology of NB is unknown, but different chromosomal (diploidy, tetraploidy, 1p deletion, 11q deletion, 14q deletion or 17q gain for example) and molecular alterations (MycN amplification, TrkA, TrkB or TrkC abnormal expressions for example) have been identified as prognostic factors [10]. The most frequent factor of a bad prognosis is MycN amplification, which occurs in 22% of NB cases [10]. Germ line mutations in *PHOX2B*, and *ALK* genes account for the majority of familial NB, while significant somatic mutation frequencies were found in *ALK*, *PTPN11*, *ATRX*, *MYCN* and *NRAS* [15-17].

At diagnosis, risk category—very low, low, intermediate or high—is established with the International Neuroblastoma Risk Group (INRG) risk classification system, which is the new classification used and defines the pretreatment group, according to stage, age, histology, tumor grade, MycN amplification, 11q aberration and ploidy [18].

INRG Stage	Age (months)	Histologic Category	Grade of Tumor Differentiation	MYCN	11q Aberration	Ploidy	Pretreatment Risk Group	
L1/L2		GN maturing; GNB intermixed					A Very low	
L1		Any, except GN maturing or GNB intermixed		NA			B Very low	
			Amp			K High		
L2	< 18	Any, except GN maturing or GNB intermixed		NA	No		D Low	
					Yes		G Intermediate	
	≥ 18		GNB nodular; neuroblastoma	Differentiating	NA	No		E Low
				Poorly differentiated or undifferentiated	NA	Yes		H Intermediate
				Amp		N High		
M	< 18			NA		Hyperdiploid	F Low	
	< 12			NA		Diploid	I Intermediate	
	12 to < 18			NA		Diploid	J Intermediate	
	< 18			Amp			O High	
	≥ 18						P High	
MS	< 18			NA	No		C Very low	
					Yes		Q High	
					Amp		R High	

Table 2: International Neuroblastoma Risk Group (INRG) Consensus Pretreatment Classification
Schema is the latest neuroblastoma classification, illustration from [18].

NB treatment can include surgery, chemotherapy, radiotherapy, biotherapy and observation alone in selected situations [7], depending on prognostic factors as shown in Table 2. For tumors with favorable biologic features, the aim is to reduce therapeutic intensity to avoid adverse side effects, whereas tumors with unfavorable prognostic factors are treated aggressively with chemo-radiotherapy [19].

Nowadays, 50 to 60% of high risk NBs are resistant to therapy [19] and hope resides in the development of new treatments targeting the molecular and genetic abnormalities responsible for the development and progression of NB. MycN amplification, which occurred in about 22% of NB cases [10] and is associated with rapidly progressive NB [20], was shown to participate in NB initiation, as transgenic mice overexpressing MycN in neuroectodermal cells developed NB [21]. Despite its potential implication in NB initiation, MycN amplification remains a controversial therapeutic target, as it is difficult to turn off an amplified gene, as opposed to a mutated gene. Moreover, a Myc inhibitor is not easy to design and the risk of adverse side effects is high considering its wide expression pattern [22]. In 2012, three targeted therapies seem promising: the radiopharmaceutical ¹³¹I-metaiodobenzylguanidine (MIBG), immunotherapy with monoclonal antibodies targeting the GD2 ganglioside and inhibitors of anaplastic lymphoma kinase (ALK) [23].

ALK gene

One of the most studied target genes in the search for new treatments for NB is the Anaplastic Lymphoma Kinase (ALK) gene. ALK was discovered in 1994, in a study about the t(2;5)(p23;q35) chromosomal translocation being responsible for ALK-NPM protein fusion in a subtype of non-Hodgkin's lymphoma [24]. Thereafter, ALK was found to be implicated in non-small cell lung cancers, retinoblastomas, melanomas, rhabdomyosarcomas, breast carcinomas, oesophageal squamous cell carcinomas [25], inflammatory myofibroblastic tumors [26] and finally sporadic and familial NB [17].

In cancer, ALK activation typically occurs by chromosomal translocation, except in NB cases where it is activated by copy number gain, gene amplification or point mutation (Figure 3). Indeed, ALK protein is expressed in 92% of NB cases [27], point mutations are present in about 6% to 11% [28] and ALK amplification was found in about 1% [28]. ALK overexpression, suspected to be associated with poor clinical outcome [29], is found in both mutated ALK and wild-type ALK. In NB with wild-type ALK gene, negative, low, moderate and high ALK immunoreactivity was shown, although molecular mechanisms of overexpression variability have not been understood yet [29]. Even though a clear association between ALK mutations and dismal prognostic NB was shown by two independent studies [30, 31], it remains controversial [28].

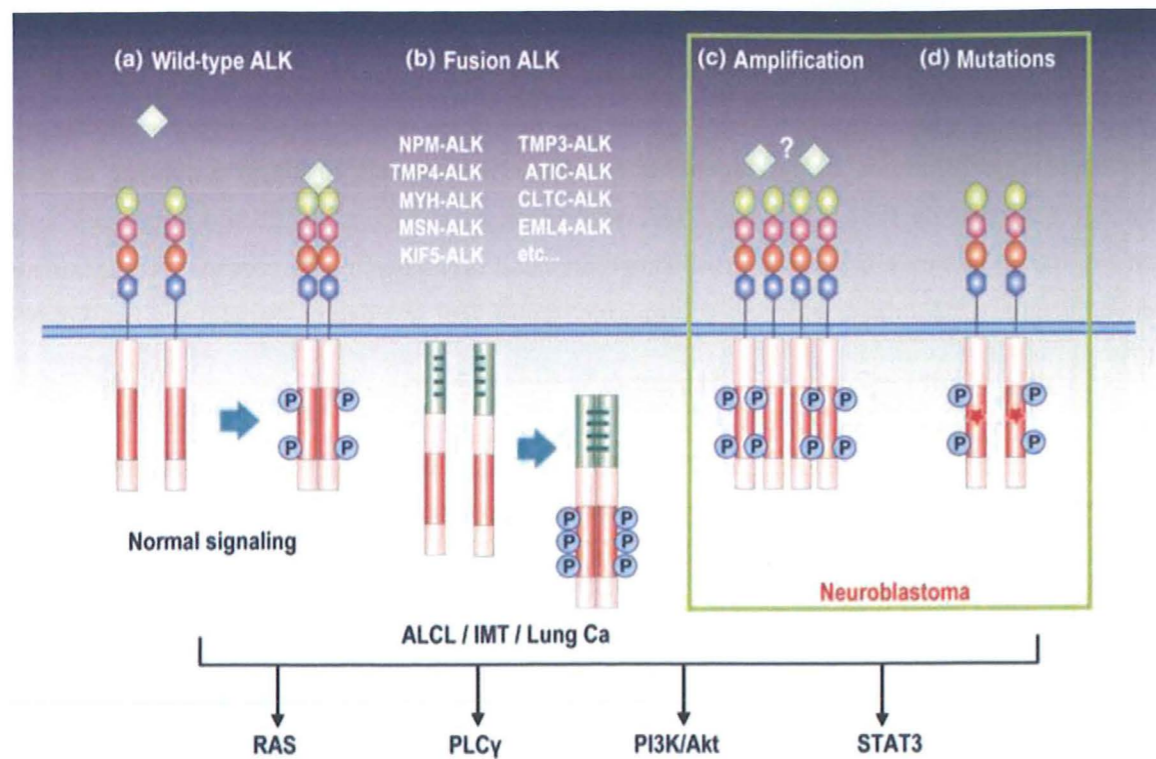


Figure 3: Physiologic and pathologic activation mechanisms of ALK, illustration from [32]. (a) Wild-type ALK activation by ligand binding. (b) Different fusion proteins with ALK are found in some cancers, such as anaplastic large cell lymphoma (ALCL), non-small-cell lung cancer (Lung Ca) and inflammatory myofibroblastic tumor (IMT). (c & d) Gene amplification or point mutation occurs in a subset of NB and induce ALK activation. Four different molecular signaling pathways have been identified with ALK activation: RAS, PLC γ , PI3K/Akt and STAT3.

ALK is located on chromosome 2p23 in humans and on chromosome 17 in mice [33]. It is a transmembranar protein of 1620 amino acid acting as receptor tyrosine kinase (RTK) [34]. ALK gene encodes for a 177 kDa polypeptide. After post-translational modifications, as N-glycosylation, a mature protein of approximately 200-220 kDa is obtained [34]. A part of full-length receptor of 220 kDa is cleaved in the extracellular domain, which creates a truncated protein of 140 kDa [35].

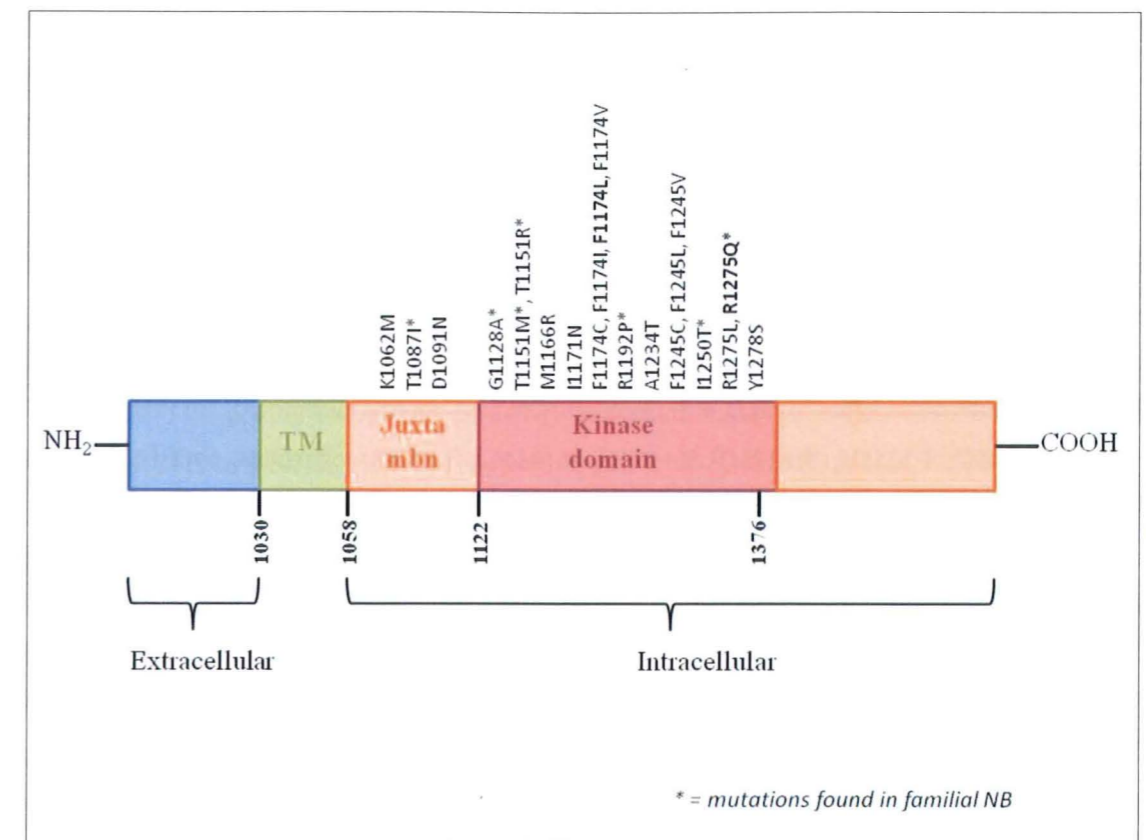


Figure 4: Structure of ALK. The most of ALK mutations are in kinase domain.

The heparin-binding growth factors Pleiotrophin (PTN) and midkine (MK) were identified as putative ALK ligands [36, 37], but binding between ALK and PTN is controversial because the interaction failed to be reproduced [34, 35]. After ligand binding induces receptor dimerization and activation via autophosphorylation [35], ALK activates different pathways of intracellular signaling molecules by phosphorylation: RAS/MAPK [38], JAK/STAT [39], PI3K/AKT [40] and PLC γ pathway [41]. These pathways, which are interconnected, are not ALK specific and can be activated by other RTKs [25].

Although the ALK gene was recently extensively studied and its expression profile suggests a role in nervous system development [42], its function is not yet fully understood. ALK mRNA is expressed in human in central and peripheral nervous system regions [24, 43] and ALK is described as having a role in neuronal differentiation [38]. In mice, its location is similar with expression starting the 11th day of embryogenesis, and declining after birth to reach low quantities in newborn [42]. In ALK knockout mice, an "antidepressant profile" was reported, with an increase in basal hippocampal progenitor proliferation and in basal dopaminergic signaling within the frontal cortex [44]. Interestingly, ALK may play a role in tumorigenicity, as it appears to be implicated in the regulation of cell survival and in apoptosis [34, 45]: in the absence of ligand, ALK seems to have a pro-apoptotic

role, while in presence of ligand or intrinsic activation it becomes anti-apoptotic, thus qualifying ALK as a dependent receptor [45]. Moreover, PTN ligand was shown to have an anti-apoptotic signaling through ALK in NIH3T3 fibroblasts [46]. Finally, MK ligand was described as “growth, survival and angiogenic factor during tumorigenesis through ALK” [37].

ALK gene mutations

The point mutations T1151M, T1151R, T1087I, R1192P, G1128A, R1275Q, I1250T, A1099T and R1464STOP have been found in germ lines [17, 30, 31, 35, 47-49], whereas in somatic lines approximately sixteen activating point mutations (F1174L, F1174C, F1174V, F1174I, A1234T, F1245L, F1245C, F1245V, R1275Q, R1275L, K1062M, M1166R, D1091N, I1171N, I1250T, Y1278S) have been described [17, 28, 30, 31, 48]. The two most frequent mutations are F1174L and R1275Q corresponding to 34.7% and 49% of mutated ALK, respectively [28]. The ALK-F1174L mutation is only present in sporadic NB cases, whereas ALK-R1245Q has been found in sporadic and familial NB cases [17, 50]. Both mutations lead to a constitutive activation of ALK protein by autophosphorylation [28], although ALK-F1174L has an increased transforming capacity compared to ALK-R1245Q [28]. Most mutations occur in the kinase domain of ALK (Figure 4), with different signaling pathways being activated depending on mutation type. For example, in Ba/F3 cells transduced with ALK-F1174L, the phosphorylated signaling molecules were STAT3 and AKT, whereas ALK-R1245Q phosphorylated efficiently ERK1/2 and AKT [48].

Cooperation between MycN and ALK

The Myc family consist of transcription factors which regulate the expression of many genes and has “roles in cell growth, proliferation, cytoskeletal structure, cellular adhesion and motility, differentiation, and apoptosis” [51]. The overexpression of Myc proto-oncogenes, such as MycN, c-Myc, and MycL, can induce a deregulation of growth and proliferation [10]. c-Myc and MycN were also shown to maintain and re-establish stem cell functions in mouse [52], and c-Myc or v-Myc is often used to immortalize neural crest stem cells [53, 54].

MycN is located on chromosome 2p24 [10], near the position of ALK at 2p23 [33]. Despite this close positioning, co-amplification of ALK and MycN is rare and observed only in unfavorable cases [55, 56], although MycN amplification is frequently associated with ALK-F1174L mutation. A meta-analysis showed 58.8% of MycN amplification associated with F1174L, against 21.6% with wild-type ALK or R1275Q mutation, and the prognostic seems to be worse with both gene alterations, than with only one [28].

ALK inhibitors

ALK is a promising therapeutic target, as its expression is not ubiquitous and it is mainly present in the neuronal system, which limits adverse side effects [25]. Moreover, immunological response against ALK should not induce a relevant autoimmune disease [25].

Crizotinib is the first drug to be approved by the US Food and Drug Administration (FDA) for treatment of ALK rearranged cancers, such as NSCLC, anaplastic large-cell lymphoma and inflammatory myofibroblastic tumor [57]. In NB cases, preclinical testing showed a good response of NB cases with ALK amplification or R1275Q mutation, but a poor response in NB with F1174L mutation [23]. One explanation is that the point mutations of ALK in its kinase domain affect ALK's 3-dimensional structure, which influences inhibitor binding [50].

In preclinical trials, the TAE-684 ALK inhibitor was shown to induce regression of murine NB initiated by ALK-F1174L in the transgenic NB mouse model, and was also effective in inhibiting tumor growth of murine NB initiated by both ALK-F1174L and MycN [58].

Aims of the project

Different chromosomal or molecular abnormalities were identified in NB, which are associated with low or high risk groups. The ALK receptor tyrosine kinase is expressed in the majority of NB: frequently overexpressed or mutated, but rarely amplified. As NB is believed to arise from primitive neural crest stem cells, we planned to investigate whether wild-type or mutated ALK in neural crest progenitor cells could drive the development of NB, and thereby determine whether ALK plays an oncogenic role in NB initiation.

In 2010, the pediatric oncology research laboratory of CHUV performed preliminary analysis using Monc1 cells [53], a neural crest progenitor cell (NCPC) line immortalized by constitutive v-Myc expression. The mutations ALK-F1174L and -R1275Q, provided by Isabelle Janoueix-Larouseix [17], were introduced in Monc1 cells by retroviral infection using the pMigr1 vector. When injected subcutaneously in nude mice, Monc1-ALK-F1174L cells rapidly gave rise to tumors, followed by Monc1-ALK-R1245Q cells, while only few mice engrafted with the negative controls Monc1 cells produced tumors with longer tumor intake.

Monc1-ALK-F1174L and Monc1 were then injected orthotopically in the adrenal glands of nude mice, which resulted in tumor growth in both groups, with faster growth present in the ALK-F1174L injected mice. Given these results, where negative controls induced tumor growth, an influence of the v-Myc oncogene—constitutively present in Monc1 cells—was suspected to take part in NCPC transformation.

For this study, we used the JoMa1 cells [54] provided by Professor Lukas Sommer. These cells were isolated from the neural crest of ROSA^{ANeo}-c-myc-ER^T transgenic mice and immortalized by an inducible c-Myc-ER. In presence of Tamoxifen, c-Myc is activated by the binding of Tamoxifen to the ER motif, allowing the translocation of c-Myc-ER into the nucleus, which ensures proliferation and maintains cells in an undifferentiated state. In absence of Tamoxifen, c-Myc is inactivated by its retention into the cytoplasm, which allows cell differentiation and avoids the side effects of c-Myc. This cell line was shown to express NCSC markers.

The aim of this study is to evaluate, *in vitro* and *in vivo*, the effect of wild-type and mutated ALK on JoMa1 cells to determine the oncogenic role of ALK in NB initiation and progression.

Materials and methods

JoMa1 cell culture

JoMa1 cells were generously given by Lukas Sommer, and were cultivated in dishes coated with 1mg/ml fibronectine (Sigma). JoMa1 medium was composed of Dulbecco's Modified Eagle Medium/F-12 (Gibco), supplemented with 1% N2-Supplement (Gibco), 2% B27-Supplement (Gibco), 0.5 ng/ml EGF (R&D), 0.2 ng/ml FGF (PeproTech), 1% Penicillin-Streptomycin (Gibco), and 10% Chicken-Embryo-Extract (CEE, produced according to [59]). For c-MycER activation, 200 nM 4-OHT (Sigma-Aldrich) was added to JoMa1 medium.

Proliferation assay by cell counting

15'000 JoMa1 cells were cultivated in 3 plates of 12-well with and without Tamoxifen. At 48, 72, and 96 hours, one of the remaining cultured plates was selected for cell counting using a counting chamber.

Proliferation assay by OD

Cells (10^3 in 100uL of JoMa1 medium) were plated in quadruplicates in 96-well plates (Corning Inc) coated with fibronectin (Sigma). Tamoxifen was added every day, diluted in 1uL of JoMa1 medium. After 0, 48, 72, and 96 hours, cell viability was assessed using the MTS/PMS cell proliferation kit (Promega). OD was measured using an ELISA reader (Dynatech MRX Microplate Reader).

JoMa1 cell transduction

ALK-wt-, ALK-F1174L-, and ALK-R1245Q-pcDNA3 constructs were generously provided by Isabelle Janoueix-Lerosey and Olivier Delattre. The ALK cDNA XhoI-EcoRI fragments were introduced into XhoI-EcoRI sites of the pMigr plasmid. The day before transduction, 2×10^6 293T cells were plated on 6-well plates in DMEM (Gibco) complemented with 10% FCS (Sigma) and 100 U/ml Penicillin-Streptomycin (Gibco). 250 μ l of a DNA solution containing 10 μ g of pMIGR vector, 10 μ g of pHit60 and 1.25 μ g of pCG was mixed with 250 μ l CaCl₂ 0.5M, and incubated at RT for 10 min. The CaCl₂/DNA mix was added to 500 μ l of HBS buffer pH 7.1 (280 mM NaCl, 10 mM KCl, 1.5 mM Na₂HPO₄-2H₂O, 12 mM Glucose and 50mM HEPES), incubated for 15 min at RT, and then added onto 293T cells. Cells were incubated at 37°C for 16 hours, after which the viral medium was replaced by fresh culture medium containing 10mM sodium butyrate (Sigma). After 8h incubation at 37°C, transfection medium was replaced by fresh JoMa1 medium and cells were incubated again for 20h at 37°C. Viral supernatant was harvested, supplemented with 1 μ l/ml polybrene (Sigma), filtrated through a 0.45 μ m filter (Milian SA) and added to JoMa1 cells—seeded in a 6-well plate one day prior—at a density of 2×10^5 cells per well. After 7h incubation of JoMa1 cells at 37°C, viral supernatant was replaced by fresh JoMa1 medium.

Flow Cytometry

JoMa1 cells were stained with anti-p75 antibody (Rabbit anti-p75 (AB1554, Millipore) and anti-rabbit antibody (AF647, LifeTechnology)) and analyzed for the expression of p75 marker by FACS (Becton Dickinson). Cells were then sorted by FACS Aria I according to GFP fluorescence.

Qualitative RT-PCR

Total RNA were extracted from cell lines using the RNeasy Mini kit (Qiagen), then quality and concentration of each RNA sample was measured by a Nanodrop (Agilent Technologies). RNA (500 ng) were reverse-transcribed to produce cDNA, using PrimeScript™ RT reagent Kit using random primer and oligo dT according to the manufacturer's instructions (TAKARA Bio Inc. Shiga). The expression levels of various genes (Table 3) were analysed by PCR using GoTaq Hot Start Kit (Promega). The cycling reactions consisted of 2min at 95°C followed by 35 cycles of 30s at 95°C, 30s at T-annealing (Table 3) and 30s at 72°C, with a final extension step of 5min at 72°C. Then, PCR reactions were loaded on 2% agarose gels. UV revelation was visualized with AlphaImager (Alpha Innotech).

	Marker	T° annealing	Primer sequences
NCSC markers	p75	65	For 5'-GAA TGC GAG GAG ATC CCT GG-3' Rev 5'-GGA GCA ATA GAC AGG AAT GAG G-3'
	Snail	60	For 5'-CAC CCA TAC AGG TGA GAA GC-3' Rev 5'-TGT CCT GGA TGA CAG AAC CA-3'
	Slug	65	For 5'-GGA GAG ACT GCA GCC CAA GC-3' Rev 5'-GTG TGC CAC ACA GCA GCC AG-3'
	Sox10	60	For 5'-CCC ACA CTA CAC CGA CCA G-3' Rev 5'-GTC GTA TAT ACT GGC TGC TCC C-3'
NB markers	Phox2b	60	For 5'-CAC CAG AGC AGT CCG TAC G-3' Rev 5'-TCT GGA ACC ACA CCT GGA C-3'
	TH	60	For 5'-ATG CTG TTC TCA ACC TGC TC-3' Rev 5'-GAA CCA GGG AAC CTT GTC C-3'
Neuronal markers	Nefh	60	For 5'-GCA GCC AAA GTG AAC ACA GA-3' Rev 5'-CTG AAT AGC GTC CTG GTA GG-3'
	Mash1	60	For 5'-TTG AAC TCT ATG GCG GGT TC-3' Rev 5'-GCC ATC CTG CTT CCA AAG TC-3'
Glial marker	GFAP	60	For 5'-ATC CCA CGT TTC TCC TTG TC-3' Rev 5'-ATC TTG GAG CTT CTG CCT CA-3'
Smooth muscle markers	Calponin	60	For 5'-GAA ATA CGA CCA TCA GCG GG-3' Rev 5'-CCA GTT TGG GAT CAT AGA GG-3'
	γ-actin	60	For 5'-GGC TTT GCA GGA GAT GAT GC-3' Rev 5'-GAG GTA GTC TGT GAG ATC CC-3'
Melanocyte marker	Tyr	60	For 5'-GTA GCA TGC ACA ATG CCT TAC-3' Rev 5'-AGA GCG GTA TGA AAG GAA CC-3'

Chondrocyte markers	Col2a	60	For 5'-TTC TGC AAC ATG GAG ACA GG-3' Rev 5'-GCT GTT CTT GCA GTG GTA GG-3'
	Sox9	60	For 5'-TGA ACG CCT TCA TGG TGT GG-3' Rev 5'-GTT CTT CAC CGA CTT CCT CC-3'
ALK	ALK human	62	For 5'-TGT TGC CTC TCC TCG ATG TG-3' Rev 5'-TGT CTT CTC CGC TAA TGG TG-3'
	ALK mouse	62	For 5'-TGC CAG AAG TGT GTT CAG AAC-3' Rev 5'-CCC TTC CAT GAA GGC TTC AG-3'
Control	G3PDH	60	For 5'-GTG AAG GTC GGT GTG AAC G-3' Rev 5'-GGT GAA GAC ACC AGT AGA CTC-3'

Table 3: Primers used for RT-PCR of transduced JoMa1 cells and subcutaneous tumors.

Real-Time PCR

The expression levels of c-Myc, MycN, and β-actin were assessed by real-time quantitative RT-PCR using the Corbett Rotor-Gene 6000 real-time cycler (Qiagen) and the Quanti Fast SYBR Green kit (Qiagen). The references of the primers used are reported in Table 4.

Primer	References
c-Myc	QT00096194, QuantiTect, Qiagen
MycN	QT00252196, QuantiTect, Qiagen
β-actin	QT01136772, QuantiTect, Qiagen

Table 4: Primers used for Real-Time PCR of JoMa1 cells

The cycling conditions comprised 5 min polymerase activation at 95°C, followed by 40 cycles of 10s at 95°C, 20s at 60°C, and 1s at 72°C for fluorescence acquisition. A standard curve was performed for c-Myc, MycN, and β-actin with serial dilutions of a reference cDNA to ensure that the amplification efficiencies were comparable. The expression levels of the c-Myc and MycN in each cell line were normalized respective to the level of the housekeeping gene β-actin. The ratio of c-Myc and MycN to β-actin gene expression was evaluated using the ΔCt method.

Immunoblotting analysis

JoMa1 cells were harvested by trypsinization, washed with PBS, resuspended in 2x pellet cells volume (PCV) of RIPA buffer and kept at 4°C. This RIPA lysis buffer was composed of 10mM NaPi buffer (pH 7.8), 60 mM NaCl, 1% Triton X100, 0.5% deoxycholic acid, 0.1% SDS, 10% glycerol, 25 mM β-glycerol phosphate, 50 mM sodium fluoride (NaF), 2 mM sodium pyrophosphate (NaPPi), 1 mM sodium orthovanadate (Na₃VO₄) and 1x Complete™ protease inhibitor (Roche). The lysates were then incubated on ice during 15 min with some vortexing and centrifugated for 15 min at 4°C at 14'000 rpm. Supernatants were removed and protein concentrations were measured with the BCA kit.

Protein extracts of 45-50µg were loaded on 7.5% or 10% SDS-PAGE and transferred on nitrocellulose membranes. Blots were blocked with 5% milk diluted in TBS-Tween20 0.1% and incubated overnight at 4°C with rabbit polyclonal antibodies specific for c-Myc (Santa Cruz Biotechnology Inc.), and ALK (Invitrogen) or mouse monoclonal antibody for β-actin antibody (Sigma). Binding of the first antibody was revealed by incubation with either goat anti-rabbit IgG-HRP or goat anti-mouse IgG-HRP (Jackson ImmunoResearch). Bound antibodies were revealed using the ECL Advanced system (GE Healthcare) or Lumi-light Western Blotting Substrate (Roche).

Phospho-immunoblotting

To obtain the protein extracts, JoMa1 cells were first resuspended in lysis buffer containing 10 mM Tris-HCl (pH 7.4), 150 mM NaCl, 5 mM EDTA, 25 mM β-glycerophosphate, 10% glycerol, 1% NP40, 0.25 % Na deoxycholate, 20 mM NaF, 1 mM Na pyrophosphate, 1 mM Na₃VO₄ and 1x protease inhibitor. Then, cell lysates were sonicated three times for 10s, and centrifuged at 13'000 rpm at 4°C during 30min. The supernatants were recovered and protein concentrations were determined with BioRad Protein Assay and aliquoted for storage at 80°C.

Protein extracts (100 ug) were separated on SDS-PAGE gels, and then transferred to Immobilon-P PVDF membranes (Millipore). Membranes were blocked for 1h in TBS-Tween 0.1% containing 2% ECL Advance™ Blocking Agent (GE Healthcare) at RT and incubated overnight at 4°C with the phospho-ALK (AssayBioTech), phospho-AKT (Cell Signaling), phospho-STAT3 (Cell Signaling) or phospho-ERK (Cell Signaling) polyclonal rabbit antibodies. Then, membranes were incubated with peroxidase Goat Anti-rabbit (Jackson ImmunoResearch) and revealed using the ECL Advanced system (GE Healthcare). Membranes were stripped 10 min at 50°C in 2% SDS, 65.5 mM Tris-HCL pH 6.8 and 100 mM β-mercaptoethanol, and finally total protein expressions were detected as loading control by the same process (ALK (Invitrogen), AKT (Cell Signaling), STAT3 (Cell Signaling), ERK (Cell Signaling)).

Sphere culture assay

JoMa1 sphere culture was performed in a neural crest stem cell medium (NCSCm), adapted from [60] and containing DMEM-F12 (Gibco) complemented with 20 ng/ml FGF-2 (Peprotech), 20 ng/ml IGF-1 (Peprotech), 1% N2-supplement (Gibco), 2% B27-supplement (Gibco), 1% Penicillin/Streptomycin (Gibco), 50 µM 2-mercaptoethanol (Merk), 35 ng/ml retinoic acid (Sigma) and 15% CEE.

10⁴ cells in 1 ml of NCSCm were cultured in PolyHema (poly (2-hydroxyethyl methacrylate), 16 mg/ml in EtOH, Sigma) coated 12-well culture plates, to prevent cell adhesion. Cells were passed every 7 days by dissociation with 0.05% trypsin-EDTA (Invitrogen) for 3.5 min and stopped with 1mg/ml Trypsin-Inhibitor (Sigma). After centrifugation, cells were resuspended in NCSCm, counted, and 10⁴ cells were plated for secondary sphere culture.

Methylcellulose 3D growth assay

JoMa1 cells were grown in a medium composed of 53% methylcellulose (Fluka, and prepared as per [61]), 17% FCS (Sigma) and 30% Dulbecco's Modified Eagle Medium (Gibco). Tamoxifen was added every two days in 100µl DMEM with 10% FCS and Penicilin-Streptomycin. After 2 weeks, cell colonies were counted using an optic microscope and colored with a mix of 50% MTS/PMS (Promega) and 50% DMEM (Gibco) during 2 hours.

Differentiation assay

10⁵ JoMa1 cells were plated per 6-well dish coated with 1mg/ml Poly-D-Lysin (Millipore) and 1mg/ml Fibronectin (Sigma), in JoMa1 medium without 4-OHT. After 24 hours, 50 ng/ml BMP2 (R&D) was added for neuronal differentiation, 34 ng/ml GGF2 (Reprokine) for glial differentiation, or 1 ng/ml TGFβ (R&D) for smooth muscle differentiation. These mediums were changed every day and after 6 days, potentially differentiated JoMa1 cells were frozen to execute a RT-PCR analysis with specific markers: Nefh and Mash1 for neurons, GFAP for glia, calponin and γ-actin for smooth muscle (Table 3).

For chondrocytes differentiation, JoMa1 cells were plated in 6-well dishes coated with fibronectine. The medium was DMEM (Gibco) supplemented with 10% FCS (Sigma), 100 U/ml Penicillin-Streptomycin (Gibco), 0.05 mg/ml Ascorbic acid (Sigma), 2 ng/ml TGFβ (R&D) and 0.1 µg/ml Dexamethasone (Sigma), and was changed every third day. RT-PCR analysis was done after 21 days with Col2a and Sox9 markers (Table 3).

In vivo studies

All animal experiments were carried out with athymic Swiss nude mice (BALB/C nu/nu) in accordance to the European Community guidelines (directive no. 86/609/CEE). For injections, mice were anaesthetized using Isoflurane (Baxter) by inhalation.

In heterotopic assays, groups of 3 mice were subcutaneously injected with a 25 G needle connected to a 1 ml syringe in both flanks with 5x10⁵ transduced JoMa1 cells in 200 ul Dulbecco modified Eagle medium (DMEM)/F12 (Gibco) and BD Matrigel™ Basement Membrane Matrix (BD Biosciences) in a 1:1 proportion.

Orthotopic injections were performed as previously described [62]. After a midline incision, 1.5x10⁵ cells in 10 µL PBS were injected in the left adrenal gland under microscope using a 28 G needle connected to a Hamilton syringe. The abdominal incision was closed with skin clips.

Tumor take and growth were followed up using calipers twice a week for subcutaneous injections and by ultrasound every 3, 7, or 14 days according to progression for orthotopic injections. Subcutaneous tumor volumes were calculated using the $(\text{length} \times \text{width}^2) / 2$ formula and orthotopic tumor volumes using formula $4 \times \pi / 3 \times (\text{depth} \times \text{sagittal} \times \text{transversal}) / 6$.

Mice with tumor volumes greater than 1000 mm³ were sacrificed.

A sample of every subcutaneous tumor was embedded in paraffin and the residual was snap-frozen into liquid nitrogen, for later protein or RNA extraction using RNeasy Mini kit (Qiagen).

Orthotopic tumors were split into four pieces: one for paraffin-embedded tissue formation, one for RNA extraction, one for protein extraction, and one for cell dissociation. Moreover, bone marrow was extracted for further analyses by flow of PBS into femoral bones using 25G needle connected to a 1 ml seringue.

Immunohistochemistry

All immuno-labelling were performed by Lausanne Mouse Pathology Facility. First, standard hematoxylin and eosin (H&E) staining was performed on all subcutaneous tumors. Secondly, three tumors per group were chosen for immunohistochemistry (IHC) with different markers (Table 5) to identify the type of tumor generated.

Antibody name	Antigen host	Cell type recognized	Source
CD44	Rat	Mesenchymal lineage, NB	550538, BD Pharmingen
NSE	Rabbit	Neuronal lineage, NB, melanoma	22521, ImmunoStar
NF	Mouse	Neuronal lineage	M0762, DakoCytomation
S100	Rabbit	Neural crest lineage	Z0311, Dako
Pax3	Mouse	Melanocyte lineage	Given by Bhushan Sarode, EPFL
Tyr	Rabbit	Melanocyte lineage	Given by Bhushan Sarode, EPFL
CD99	Rabbit	Ewing sarcoma	Orb13719, Biorbyt
NCAM1 =CD56	Rabbit	NB	14255-1-AP, Proteintech
TH	Mouse	Dopaminergic and noradrenergic neurons, NB	MAB318, Millipore
Synaptophysin	rabbit	Neurosecretory vesicles, including presynaptic vesicles	Ab23754, abcam
ALK (Tyr1604)	rabbit		Invitrogen

Table 5: Antibodies used for IHC of subcutaneous tumors

Statistical analysis

Statistical significance of the results was analysed using t-test, one-way ANOVA or two-way ANOVA analysis using GraphPad Prism 5.04 software (GraphPad Software, Inc.).

Results

Switch of c-MycER

Western-Blot of c-MycER

JoMa1 cells express a c-MycER, which is activated by Tamoxifen. The active form of c-MycER translocates into the nucleus to regulate genes expression, whereas the inactive form stays in cytoplasm. To check the switch of c-MycER from the active to the inactive configuration, nuclear and cytoplasmic proteins were extracted from JoMa1 cells treated with and without Tamoxifen and c-MycER localization was analyzed by Western-Blot (Figure 5).

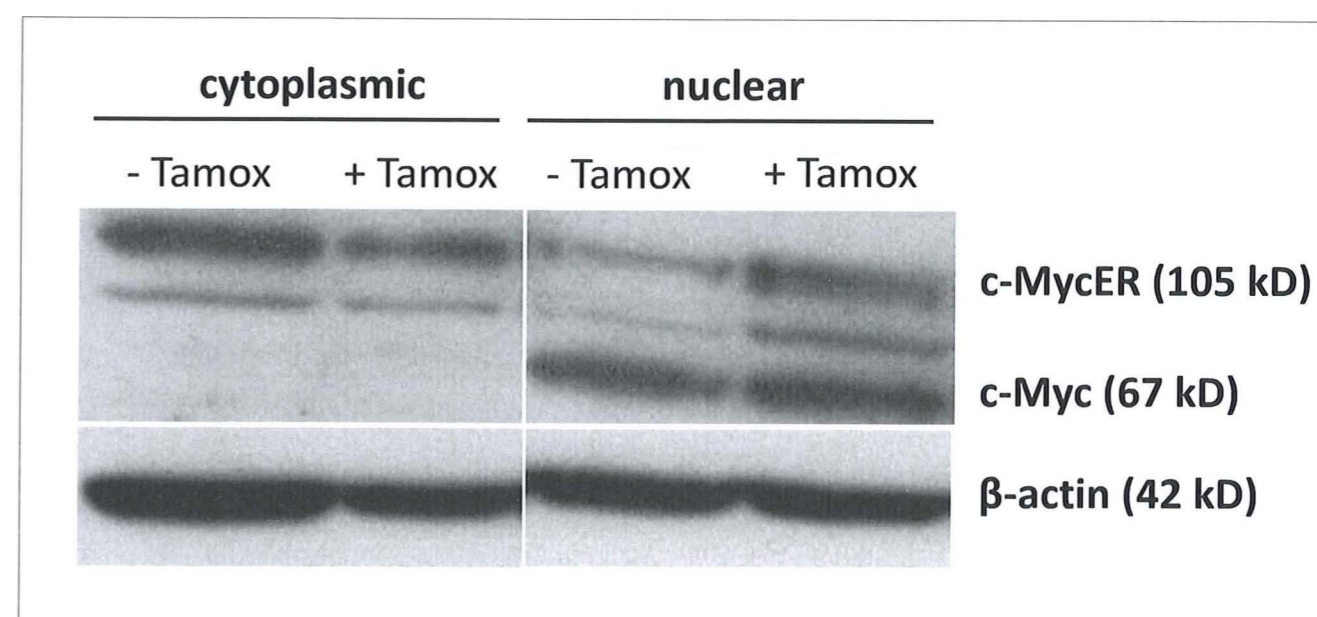


Figure 5: Western-Blot of c-MycER. "- Tamox" = JoMa1 cells cultured without Tamoxifen during 5 days, "+ Tamox" = cells cultured with Tamoxifen. β -actin was used as loading control.

In the presence of Tamoxifen, the c-MycER protein was observed in the nucleus and in the cytoplasm; whereas in the absence of Tamoxifen, c-MycER protein decreased in the nucleus. This means that the inactive form is not transported into the nucleus and thus remains inactive. Endogenous c-Myc expression was a little higher in the nucleus in presence of Tamoxifen, suggesting a weak effect of c-MycER activation on endogenous c-Myc expression.

Growth assay

A proliferation assay was performed to highlight the effect of c-MycER activation on cell proliferation, which should be increased in presence of Tamoxifen. As illustrated in Figure 6, JoMa1

cells cultured with Tamoxifen grew faster than those without Tamoxifen. The difference became visible after about 48 hours, and at 96 hours there were four times more cells in presence of Tamoxifen. This also shows that c-MycER inactivation by Tamoxifen withdrawal impaired JoMa1 cell proliferation, as expected.

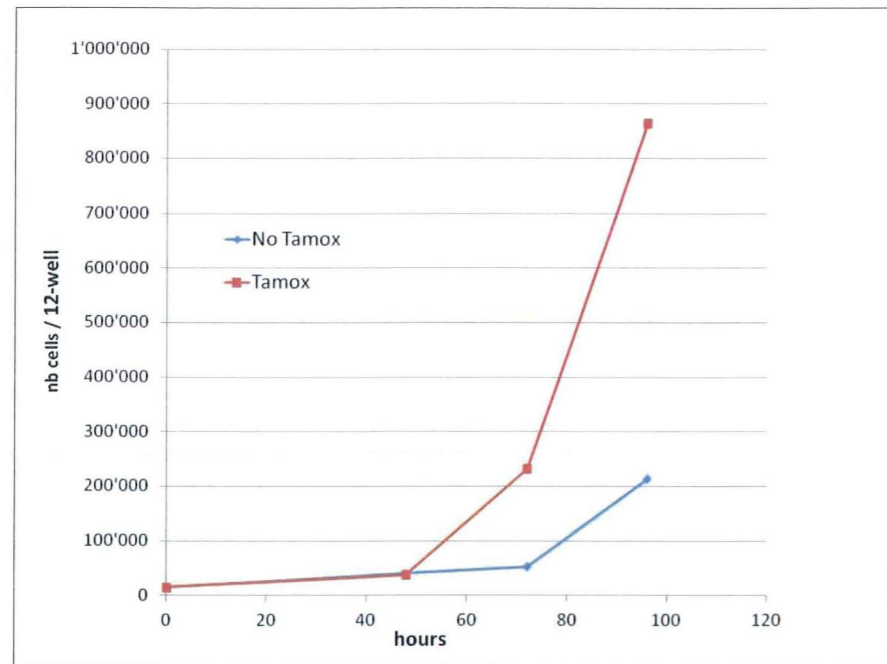


Figure 6: Proliferation assay by cell counting. "No Tamox" = cells cultured in absence of Tamoxifen from time 0, "Tamox" = cells cultured with Tamoxifen.

Transduction of JoMa1 cells

Cell sorting of transduced cells

ALK-wt, ALK-F1174L, and ALK-R1245Q were stably overexpressed in JoMa1 cells by retroviral infection using the pMigr1 vector, which encodes for the Green Fluorescent Protein (GFP). Transduction efficiency was analyzed by measuring the percentage of the GFP positive cells by FACS. In addition, the expression of the NCSC marker p75 was measured to ensure that transduced cells remained undifferentiated. The FACS analyses (Figure 7) showed that most cells were p75 positive and that between 91% and 58% of cell populations were transduced. P75+ cell sorting was therefore not necessary, but the GFP positive JoMa1 cells were sorted by FACS, to get pure populations of transduced cells. After cell sorting, another FACS for GFP expression showed that cell populations were enhanced in transduced cells with new percentages between 90.7% and 97.2%. Thus, almost pure populations of transduced JoMa1 cells expressing the p75 NCPC marker were obtained.

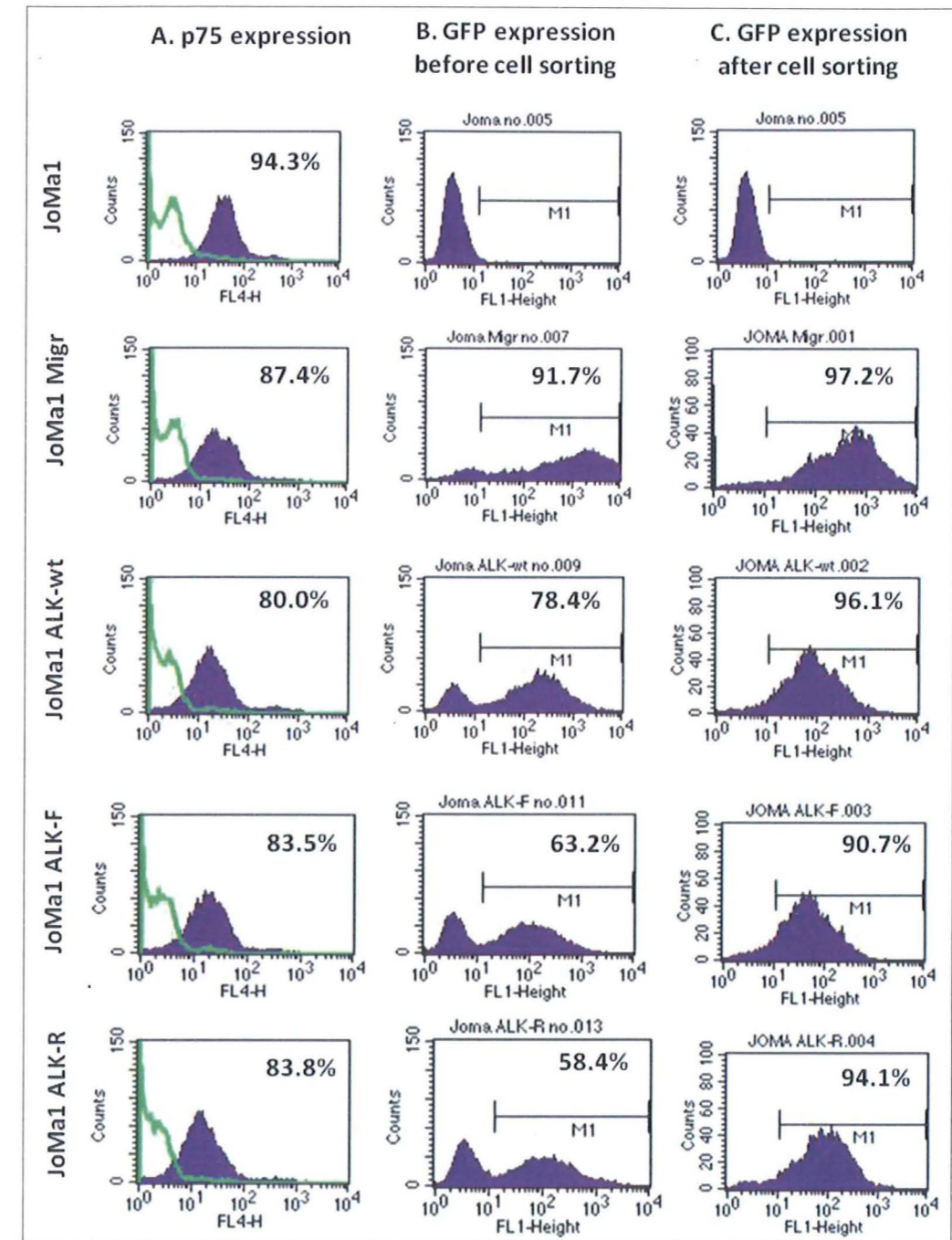


Figure 7: (A.) p75 expression in transduced JoMa1 cells. (B.) GFP expression in transduced cells before cell sorting. (C.) GFP expression in transduced cells after cell sorting.

ALK expression in transduced cells

The next step was verifying the ALK mRNA and protein expression by RT-PCR and Western-blot, respectively. As shown by RT-PCR (Figure 8A), ALK mRNA was present in ALK-wt, ALK-F1174L, and ALK-R1245Q JoMa1 cell lines. ALK protein was also produced by these cell populations, as observed by Western-Blot (Figure 8B). The presence or absence of Tamoxifen did not affect ALK mRNA and protein expressions. But interestingly, ALK-wt seemed to be expressed as strongly as mutated ALK. Thus, transduced cells stably express wild-type and mutated ALK proteins.

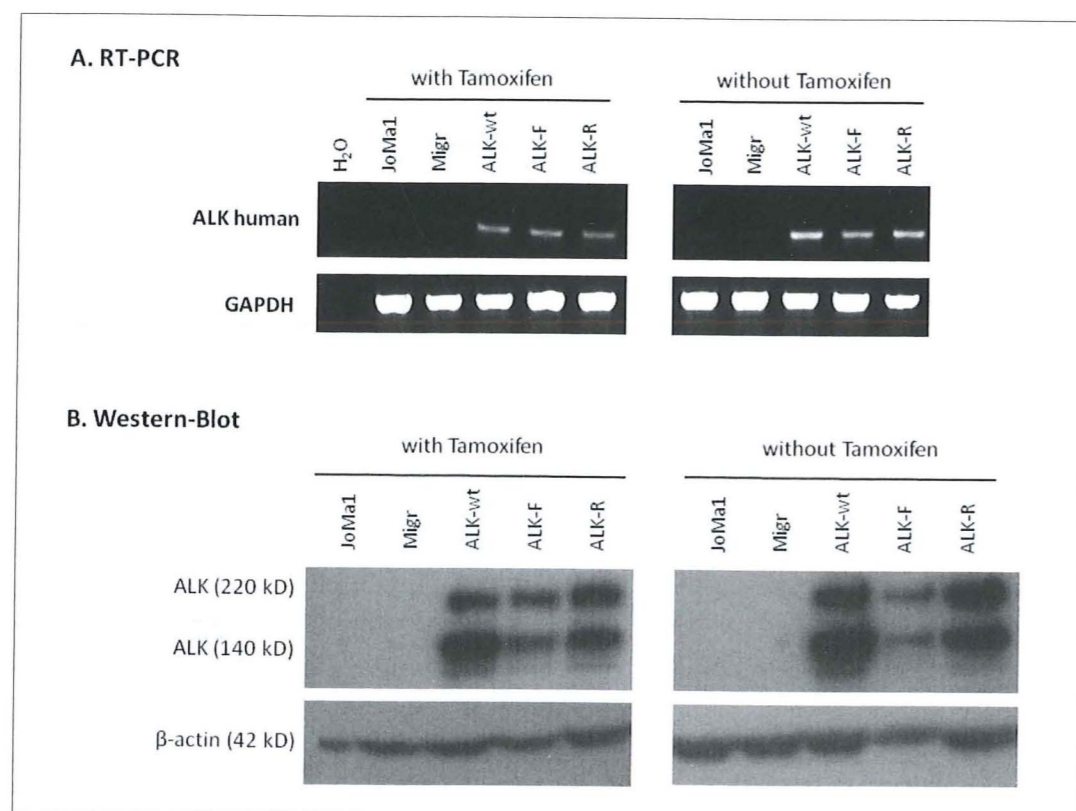


Figure 8: (A.) Detection by RT-PCR of ALK mRNA in transduced cells cultured with and without Tamoxifen for 72 hours. GAPDH was used as internal control. (B.) Detection by Western-Blot of ALK protein in transduced cells cultured with and without Tamoxifen for 96 hours. β-actin was used as loading control.

Characteristics of transduced JoMa1 cells

RT-PCR

We analyzed the phenotype of the transduced JoMa1 cells by RT-PCR. Different markers were used to ensure NCPC phenotype, such as the early neural crest marker p75, and the genes associated with neural crest induction Sox 10, Slug, and Snail [63-65]. We also used different markers for cells types which can be derived from NCPC, such melanocyte, chondrocyte, neuron, smooth muscle, glia and NB to test their state of differentiation.

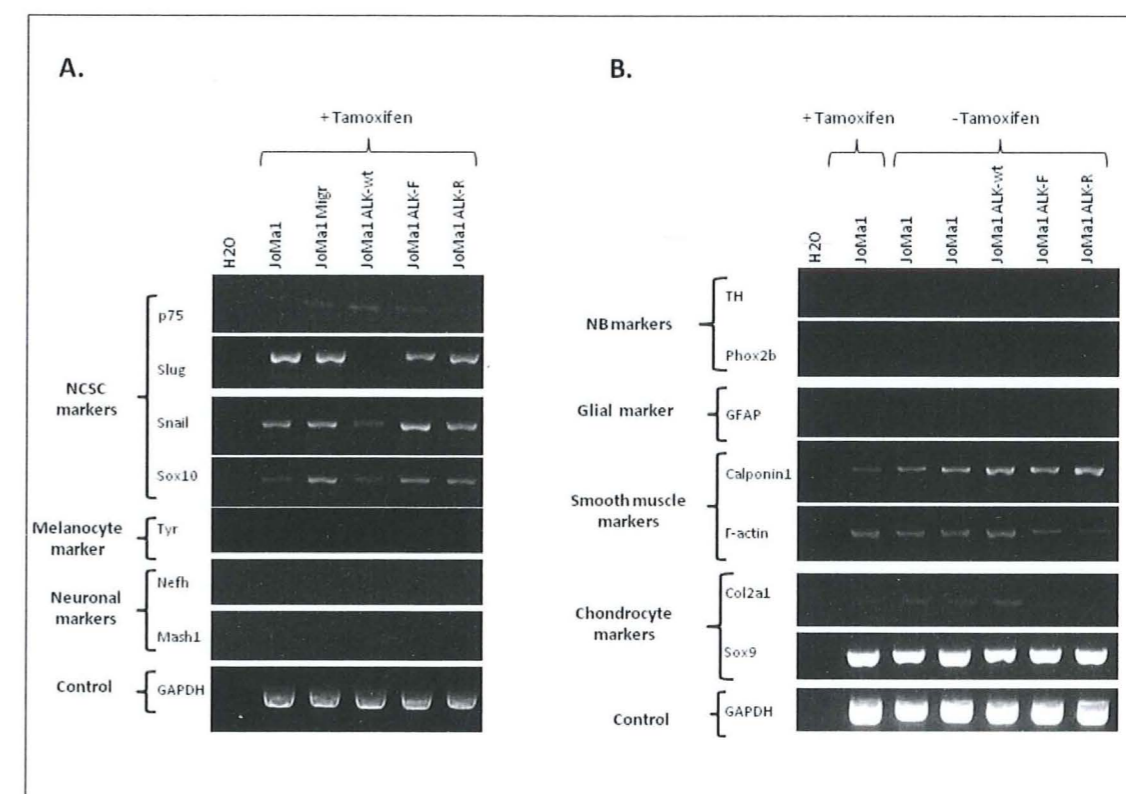


Figure 9: Expression levels of various NCSC and differentiation markers analyzed by RT-PCR in total RNA from JoMa1 parental and transduced cells treated with Tamoxifen (A) or without Tamoxifen (B).

As shown in Figure 9, the NCPC markers expression was variable in each cell line, except Slug in JoMa1-ALK-wt cells which was not expressed. Melanocyte, neuron, glia, and NB markers were not detectably expressed. Smooth muscle and chondrocyte markers were found in transduced JoMa1 cells, but also in the parental JoMa1 cell line, which means that JoMa1 cells already presented these differentiation markers.

Differentiation test

As JoMa1 cells are NCPC, they should display some pluripotential abilities. Parental JoMa1 cells were tested first to verify differentiation capacity of the parental cell line. To assay for this property, BMP2 was added to the JoMa1 medium during six days to induce neuronal differentiation, GGF2 was added for glial differentiation, TGF β for smooth muscle induction, and a special medium for chondrocyte transformation. Morphology changes were photographed with an optical microscope (Figure 16) and differentiation markers were assayed by RT-PCR (Figure 17).

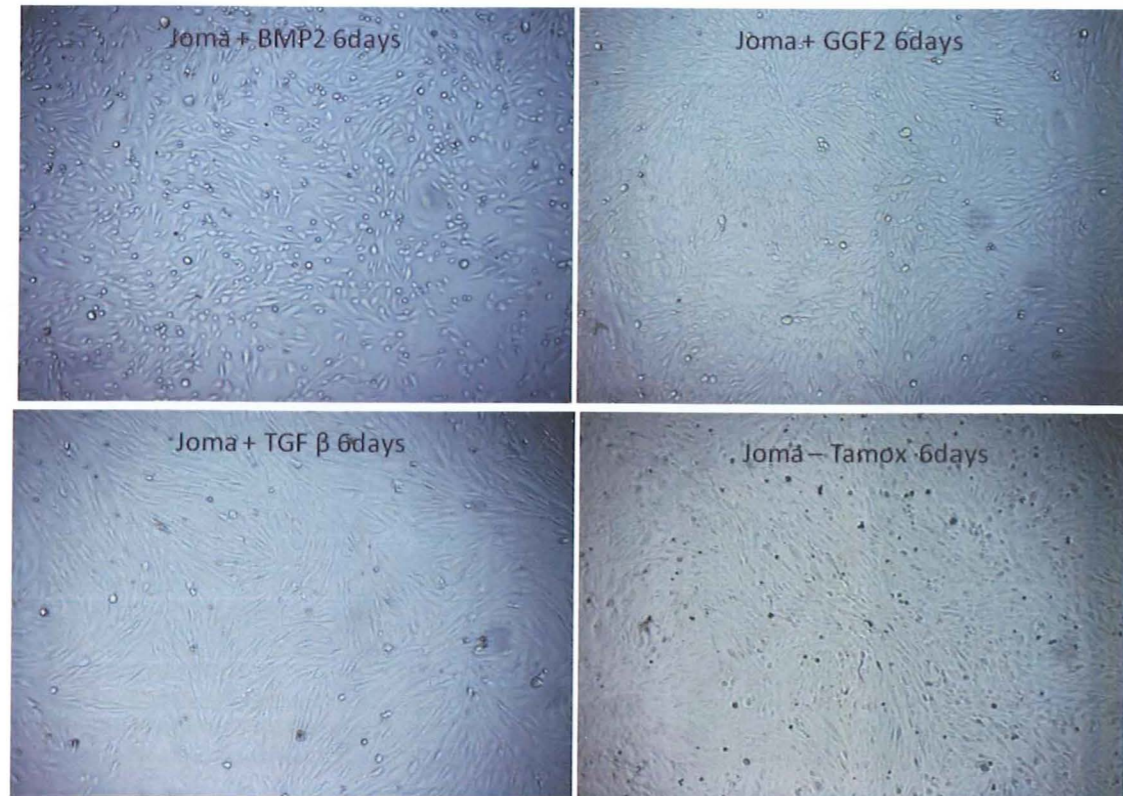


Figure 16: Differentiation assay. Pictures of differentiated JoMa1 cells taken after 6 days of induction with BMP2, GGF2, TGF β , and in absence of Tamoxifen as control.

The most important morphologic change occurred after TGF β induction, where cells became long and slender (Figure 16). The chondrocyte medium induced non adherent, floating, round and small cells (not shown).

After 6 days of differentiation induction, NCSC marker expression was expected to decrease while differentiation markers should appear in their respective differentiation pathways. As illustrated in Figure 17, a weak decrease in NCSC markers occurred for p75 with TGF β induction, for Snail with BMP2 and TGF β induction, and in Sox10 with BMP2 induction. The glial marker GFAP was not detectable. For neuronal markers, Mash1 was only expressed in JoMa1 cells without induction and

Nefh appeared as much in the absence of Tamoxifen as with BMP2 and GGF2 induction. Smooth muscle markers (Calponin1 and γ -actin) were already present in parental JoMa1 cells and no increase could be detected by RT-PCR. For chondrocyte induction, no sufficient RNA could be obtained for RT-PCR analyses. Therefore, RT-PCR results did not highlight a significant increase in any differentiation markers to confirm differentiation in one pathway.

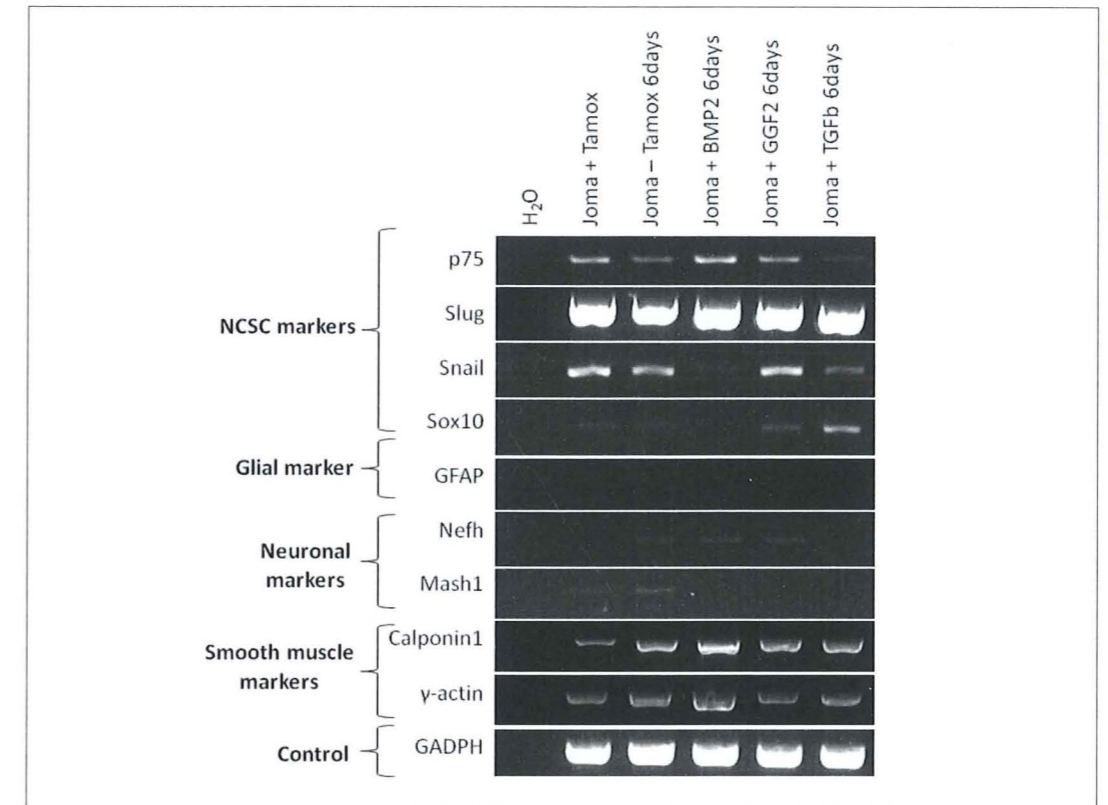


Figure 17: Expression levels of various NCSC and differentiation markers analyzed by RT-PCR in total RNA from parental JoMa1 cells treated with or without Tamoxifen or induced for differentiation by BMP2, GGF2, TGF β for 6 days.

Endogenous expression of c-Myc and MycN

To see whether there was an influence of c-MycER system on endogenous c-Myc expression, and whether the MycN expression level was influenced by c-MycER expression or ALK mutations, endogenous MycN and c-Myc mRNA expression levels were measured by Real-Time PCR, as shown in Figure 10.

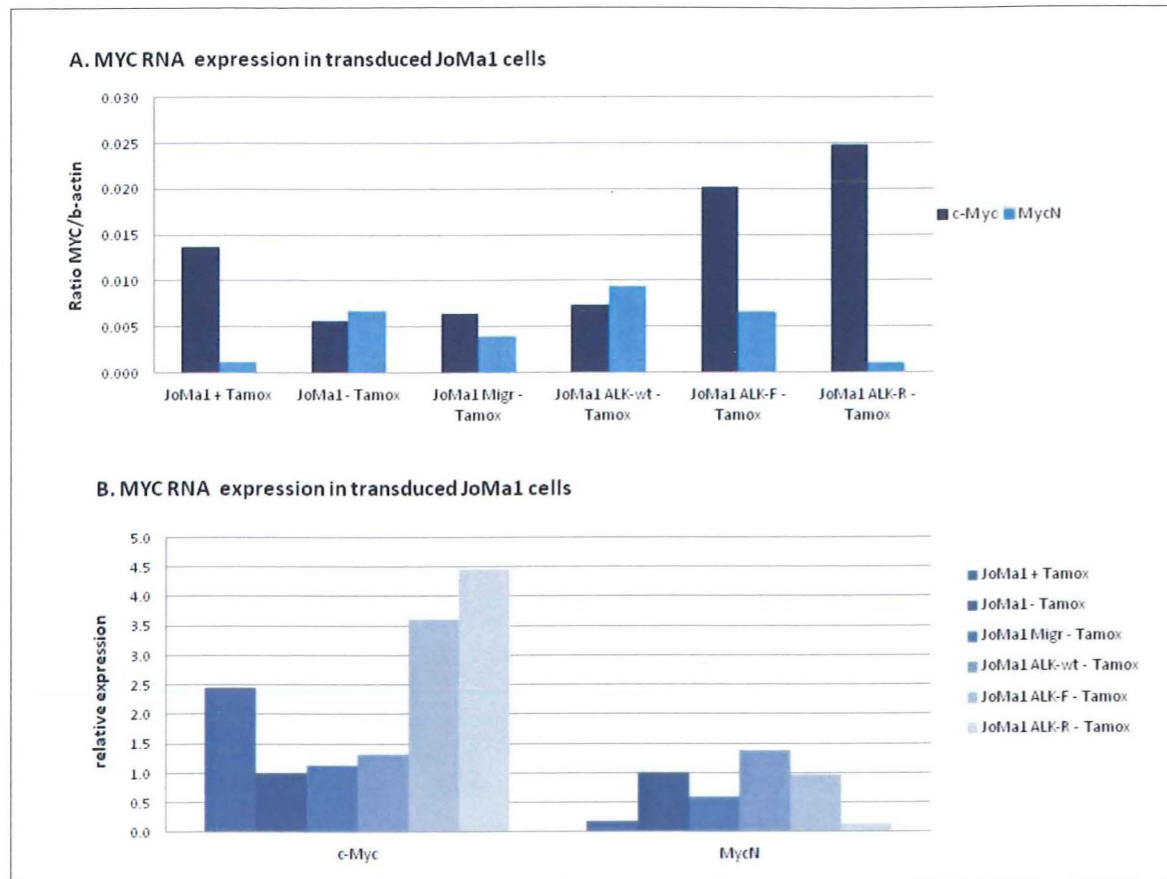


Figure 10: Expression level of endogenous *c-Myc* and *MycN* mRNA measured by Real-Time PCR. (A.) The bar graph represents the ratio between [*c-Myc* or *MycN*] and β -actin expression. (B.) The relative expression of *c-Myc* and *MycN* according to JoMa1 without Tamoxifen are plotted. JoMa1 and transduced cells were cultured for 4 days in absence (-) or in presence (+) of Tamoxifen (Tamox) before RNA extraction.

We used a mouse primer to detect endogenous *c-Myc*, so human *c-MycER* should not be detected. Our results show that *c-Myc* was about 2.5 times more expressed in non-transduced JoMa1 cells treated with Tamoxifen than without Tamoxifen. *c-Myc* expression also increased in presence of ALK-F1174L and ALK-R1245Q mutants from 3.5 to 4.5 times, respectively, and compared to non-transduced JoMa1. Here, an influence of *c-MycER* was excluded because these groups were cultured without Tamoxifen, so it could be attributed to ALK mutations.

The ratio of *MycN*/ β -actin was weaker compared to *c-Myc*/ β -actin ratio, and didn't exceed 0.015. *MycN* expression seemed to be inversely correlated with *c-Myc* expression and thus *MycN* expression was reduced when *c-Myc* was highly expressed in parental JoMa1 cells with Tamoxifen and in ALK-R1245Q JoMa1 cells, but not in ALK-F1174L JoMa1 cells.

Activation of ALK signaling pathways

Previous study has shown that ALK-F1174L and ALK-R1245Q were constitutively activated by phosphorylation [28]. To analyze the three major signaling pathways activated by ALK in JoMa1 cells, we measured the phosphorylation of Stat3, AKT and ERK by Western-Blot in protein lysates from transduced and parental JoMa1 cells with and without Tamoxifen (Figure 11).

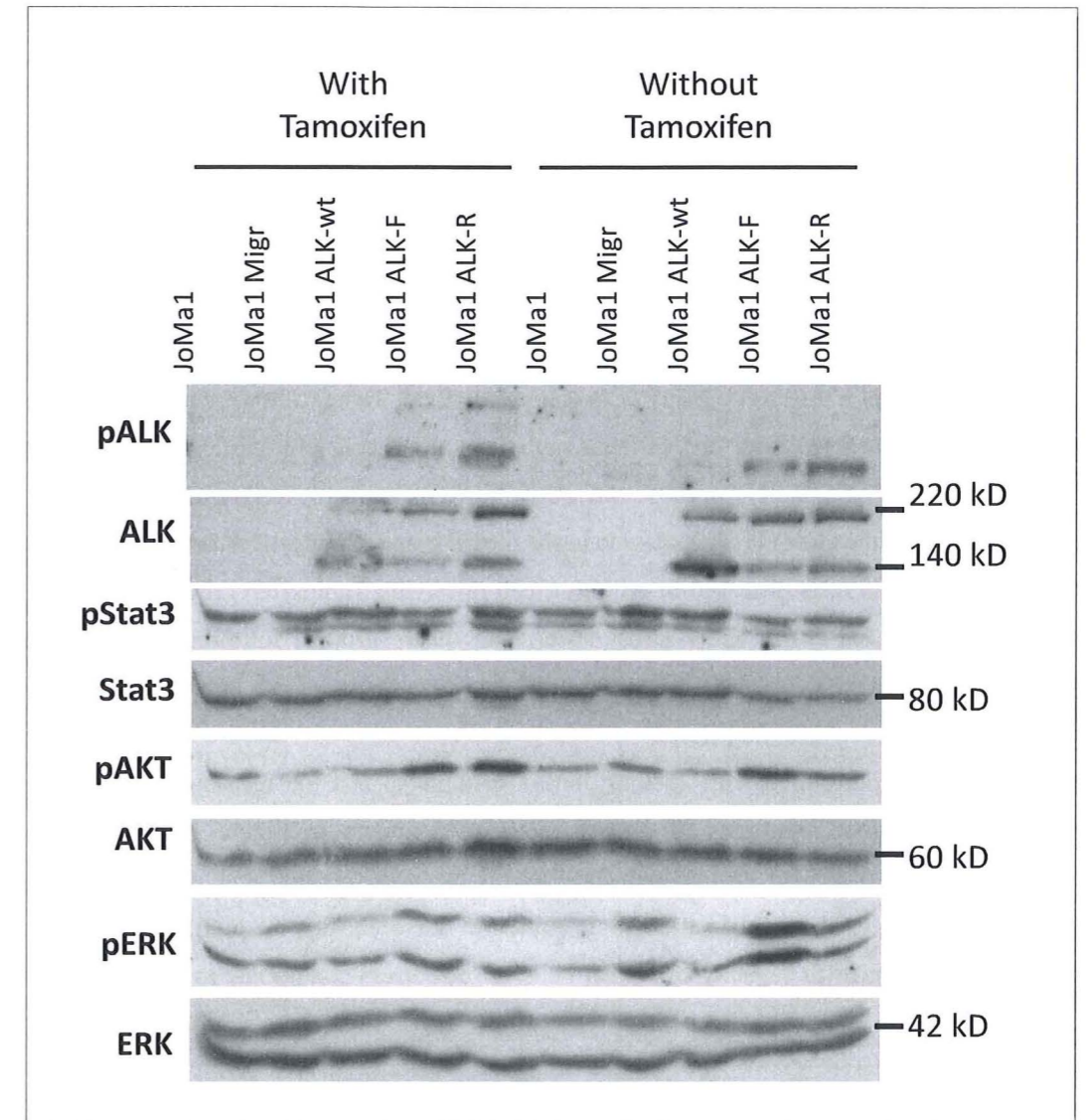


Figure 11: Phospho-Western-Blot of *pALK*, *pStat3*, *pAKT*, and *pERK* in parental and transduced JoMa1 cells. Total *ALK*, *Stat3*, *AKT*, and *ERK* proteins were used as loading controls.

Both isoforms (140 and 220 kD) of ALK protein were present in the ALK-wt, ALK-F1174L, and ALK-R1245Q cell lines. Phosphorylated ALK protein was detected in ALK-F1174L, ALK-R1245Q, and weakly in ALK-wt cells, for the 140kD isoform both in presence and absence of Tamoxifen. The

220kD isoform was only weakly phosphorylated in ALK-F1174L and ALK-R1245Q JoMa1 cells with Tamoxifen. AKT seemed to be more phosphorylated in ALK-F1174L and ALK-R1245Q cell lines with Tamoxifen and in ALK-F1174L without Tamoxifen. Phospho-ERK was only enhanced in ALK-F1174L without Tamoxifen. While Stat3 was already highly phosphorylated in parental and JoMa1-Migr control cells, no increase in phosphorylation could be observed in ALK expressing cells. Thus, constitutively activated ALK-F1174L activates the AKT and ERK pathways in JoMa1 cells, while ALK-R1245Q shows a preferential activation of AKT pathways, but only in presence of Tamoxifen. This also indicates that human ALK-F1174L and ALK-R1245Q mutants are functional and able to activate downstream signaling pathway in murine cells.

In vitro assays with transduced JoMa1 cells

Growth assays

Proliferation assays of transduced JoMa1 cells with and without Tamoxifen were performed to analyze whether the presence of ALK or one of these mutations affect cell proliferation. The four executed tests were not really comparable because the values were inexplicably very different between tests, which explains why the error bars are so wide in the means graph (Figure 12 A. and B.). That said, this graph shows the main facts observed in each test: cell lines with Tamoxifen grew faster than without Tamoxifen, and ALK-F1174L grew much faster than others groups, followed by Migr, parental JoMa1, ALK-wt, and ALK-R1245Q.

The same test was performed with 25% of JoMa1 medium to test the resistance of cells to stress conditions, with reduced amounts of growth factors. As shown in Figure 12 (C. and D.), the proliferation pattern of JoMa1 groups with 25% JoMa1 medium was the same as with 100% JoMa1 medium. Surprisingly, the proliferation was higher in 25% JoMa1 medium, which indicates a generally increased growth capacity of JoMa1 cells in such stress conditions, as measured within 96 hours.

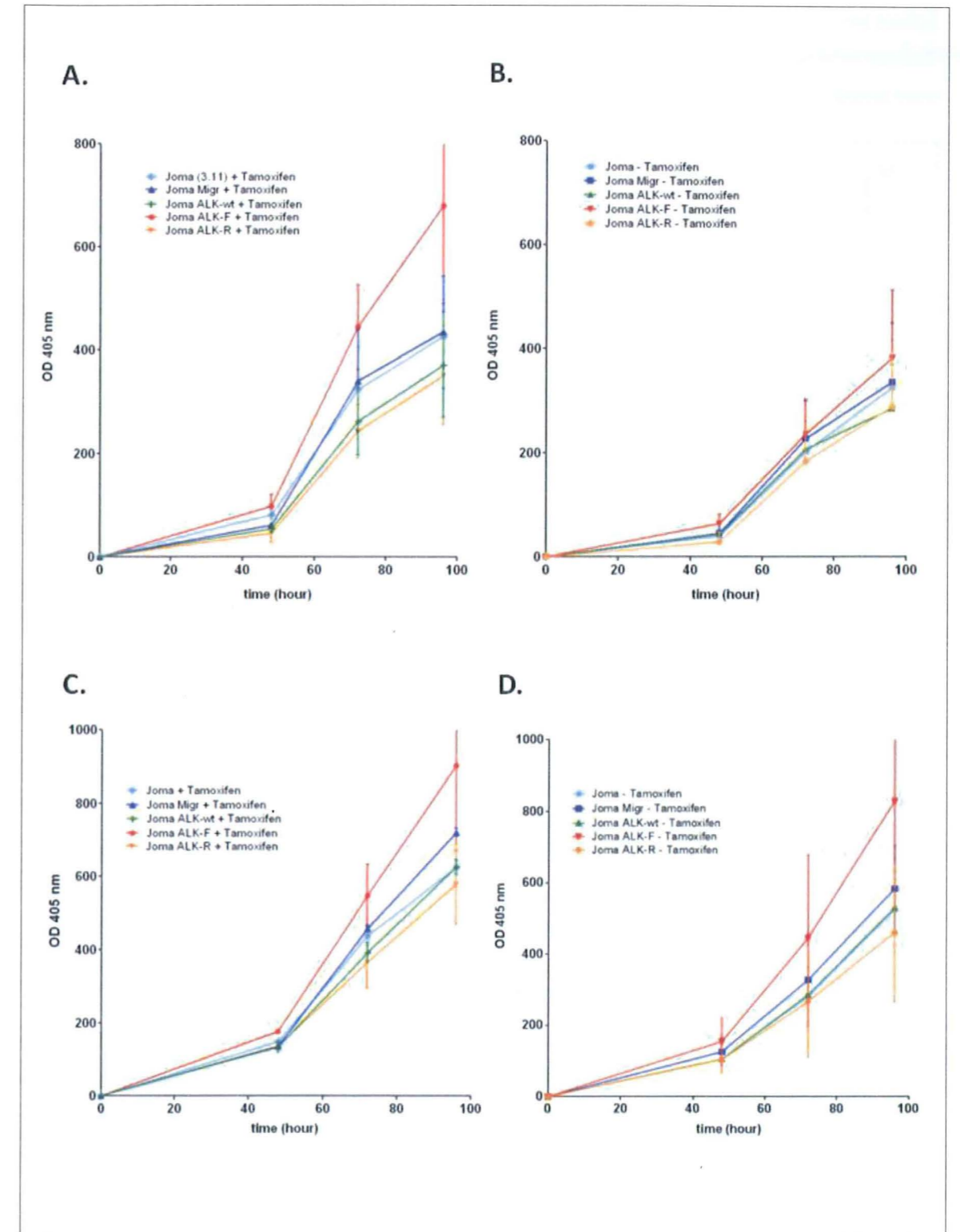


Figure 12 : Mean of four transduced JoMa1 cells proliferation assays in 100% JoMa1 medium with (A.) and without (B.) Tamoxifen. Mean of two transduced JoMa1 cells proliferation assays in 25% JoMa1 medium, with (C.) and without (D.) Tamoxifen.

Sphere assays

The self-renewal and proliferation capacities of JoMa1 transduced cells in non adherent conditions were tested by performing sphere assays.

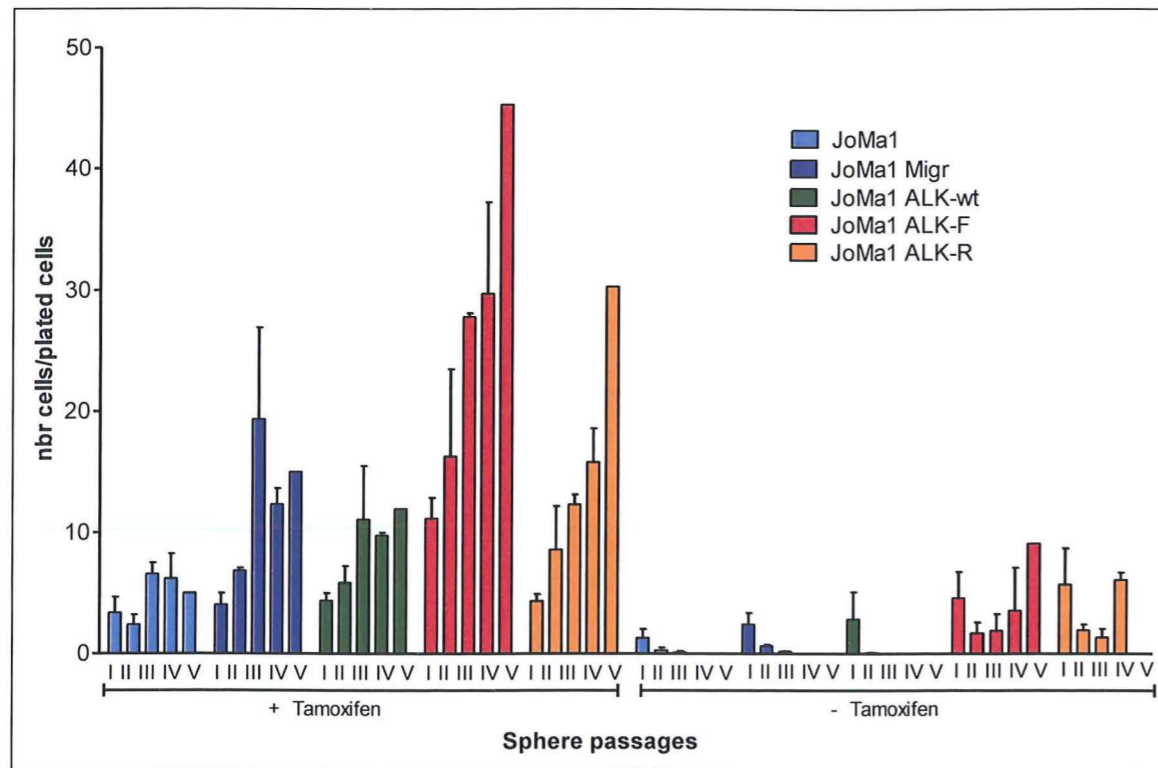


Figure 13: The graph represents the sphere-forming capacity of JoMa1 and transduced cells cultured in presence or absence of Tamoxifen for up to five sphere passages (I to V). Mean of two sphere assays, except for passage V, where only one value per cell line was available. To obtain sphere-forming capacity, the number of cells counted after one week in culture was divided by the number of plated cells.

In absence of Tamoxifen, cells were unable to be maintained over passage II or III, except for ALK-F1174L- and ALK-R1245Q-expressing cells. In presence of Tamoxifen, all cell lines displayed sphere forming capacities over five passages. In each sphere passage, ALK-F1174L had the highest sphere forming capacity, but the difference between each cell line was the greatest at the Vth passage with ALK-F1174L as the highest, followed by ALK-R1245Q, Migr, ALK-wt, and not-transduced JoMa1. Interestingly, ALK-F1174L and ALK-R1245Q JoMa1 cells showed an enhanced capacity to proliferate in sphere assays, as their sphere forming capacities increased along with sphere passages (Figure 13).

Methylcellulose 3D growth assay

To assay the tumorigenic capacity of transduced JoMa1 cells *in vitro*, culture in a semi-solid medium (methylcellulose) was performed. This test allows a prediction of future *in vivo* assays.

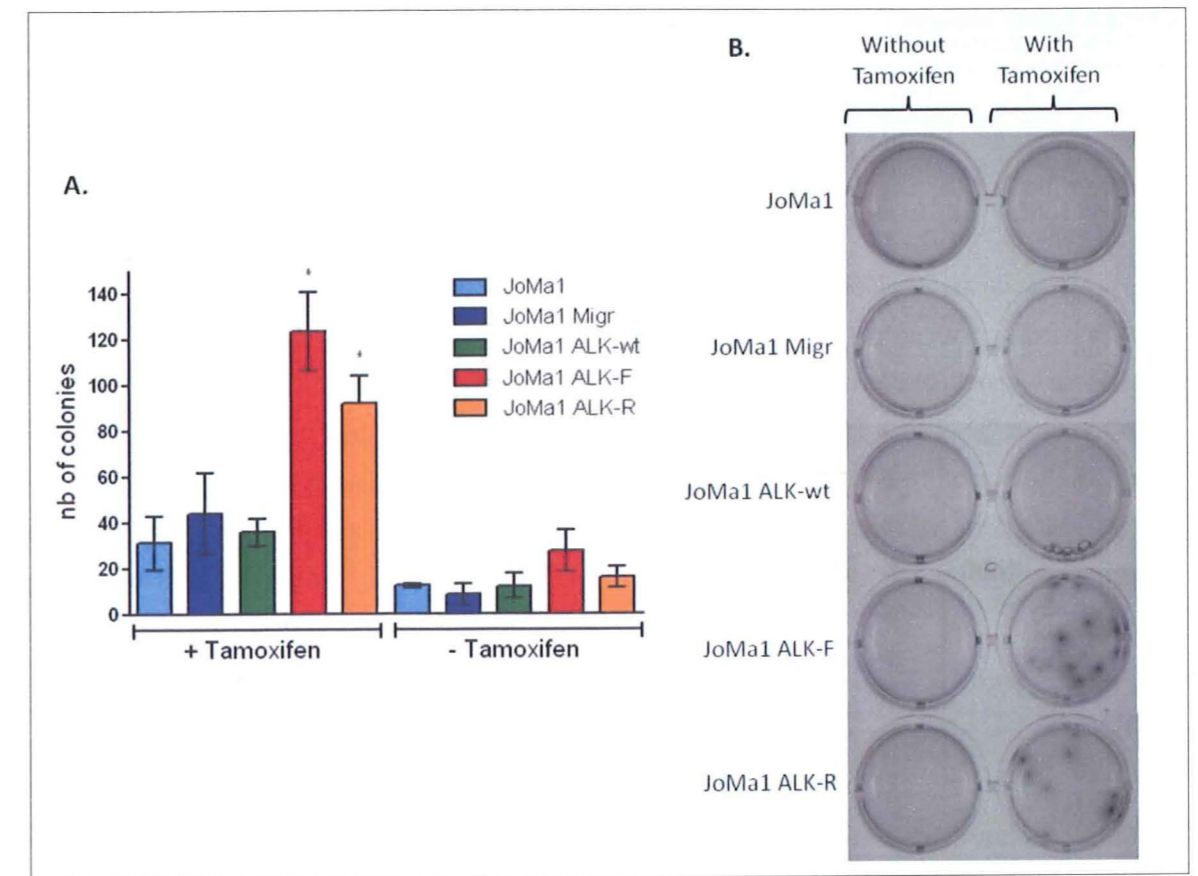


Figure 15: (A.) Mean of three methylcellulose assays. (B.) Pictures taken with AlphaImager® of one representative methylcellulose test colored by MTS/PMS reagent.

As shown in Figure 15, methylcellulose assays showed that while JoMa1 parental, Migr, and ALK-wt cells displayed similar clonogenic capacity, significantly more colony formation was observed with Tamoxifen in ALK-F1174L- and ALK-R1245Q-expressing cells than in Migr control cells. Moreover, colony size was larger in ALK-F1174L and ALK-R1245Q groups, macroscopically detectable after staining by MTS/PMS reagent. In the absence of Tamoxifen, all cells were only able to form few microscopic colonies. In conclusion, ALK-F1174L and ALK-R1245Q cell lines displayed the higher oncogenic capacities *in vitro* and so were expected to be tumorigenic *in vivo*.

In vivo assays with transduced JoMa1 cells: subcutaneous and orthotopic injections

Subcutaneous implantations

To analyze the tumorigenic effect of ALK-wt and mutants *in vivo*, transduced JoMa1 cells were first subcutaneously implanted in nude mice. Subcutaneous implantations are generally more permissive, less invasive, and cheaper than orthotopic implantations, so subcutaneous injections were performed to screen *in vivo* cell growth in nude mice. To analyze the oncogenic role of ALK independently of c-MycER activity, no Tamoxifen was given to the mice. As negative controls, we used parental JoMa1 cells and JoMa1 cells transduced only with pMigr vector, in order to rule out a potential effect of the vector.

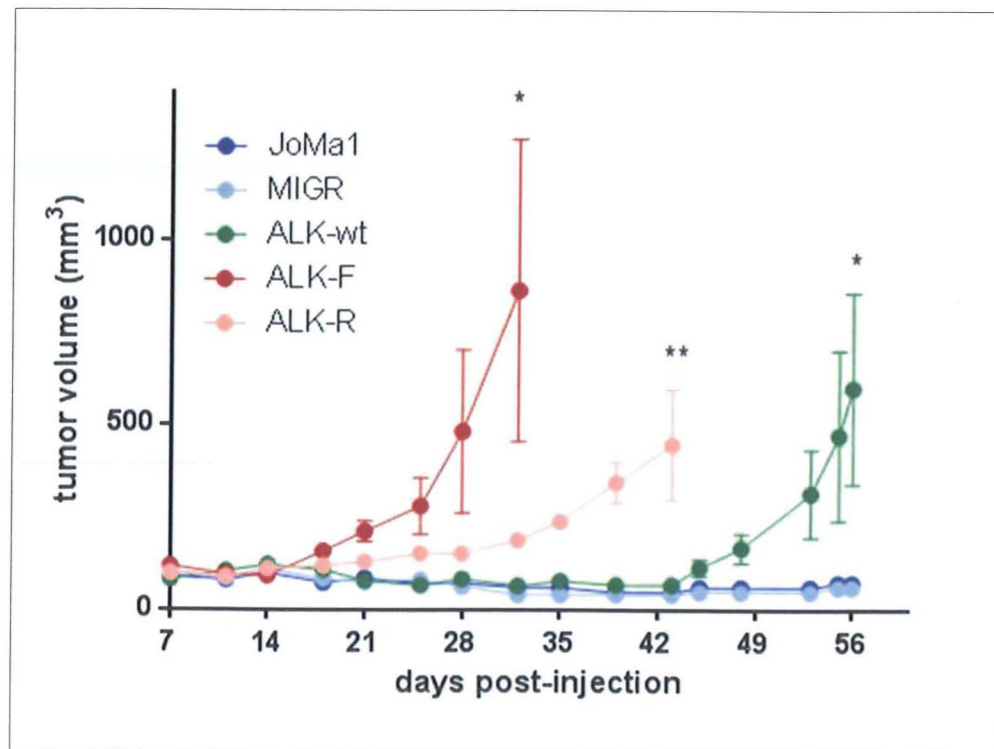


Figure 18: Tumor growth in heterotopic model. Mice were sacrificed once tumor volume reached 1000mm³. Mean tumor volume by groups are plotted from first measures made 7 days post-injection, until the first mice of the group had to be sacrificed. The basal volume of 40-125mm³ was caused by MatrigelTM, a gelatinous mixture in which cells were injected subcutaneously to avoid cell dissemination. The remaining control mice were sacrificed 60 days post-injection.

As shown in Figure 18, ALK-F1174L-derived tumors displayed a highly rapid growth, as tumors reached a mean volume of 450 mm³ in 28 days. ALK-R1245Q- and ALK-wt-derived tumors developed slightly less rapidly and reached 450 mm³ after 43 and 55 days, respectively. In ALK-

F1174L and ALK-R1245Q groups, 6/6 (100%) mice developed tumors, while 4/6 (67%) did so in the ALK-wt group. Interestingly, the control groups implanted with JoMa1 and JoMa1-Migr cells did not induce tumor formation, indicating that tumor growth resulted from ALK expression.

RNA was extracted from three tumors per group to attempt to characterize tumor type by RT-PCR, as shown in Figure 19. The results of the three groups were compared. NCSC markers were expressed in all groups. The p75 marker seemed to be weaker and Snail stronger in ALK-F1174L group than in other groups. Sox10 signal was higher in ALK-F1174L and ALK-R1245Q groups. The differentiation markers did not bring out a clear NB profile. Neuronal markers appeared more or less strongly in most tumors (Nefh in 6/9 tumors and Mash1 in 8/9 tumors). Surprisingly the melanocyte marker (Tyr) was expressed in one ALK-R1245Q tumor. For NB markers, only one ALK-wt tumor expressed Phox2b. GFAP, a glial marker, was not detected in any tumor. Smooth muscle markers (Calponin1 and γ -actin) were more strongly expressed in about three ALK-wt tumors and two ALK-R1245Q tumors. Col2a1 and Sox9, which are expressed in chondrocytes, were strongly expressed in all tumors. ALK human was expressed in all tumors with the same signal. Thus, it was not possible to confirm the NB phenotype of these tumors.

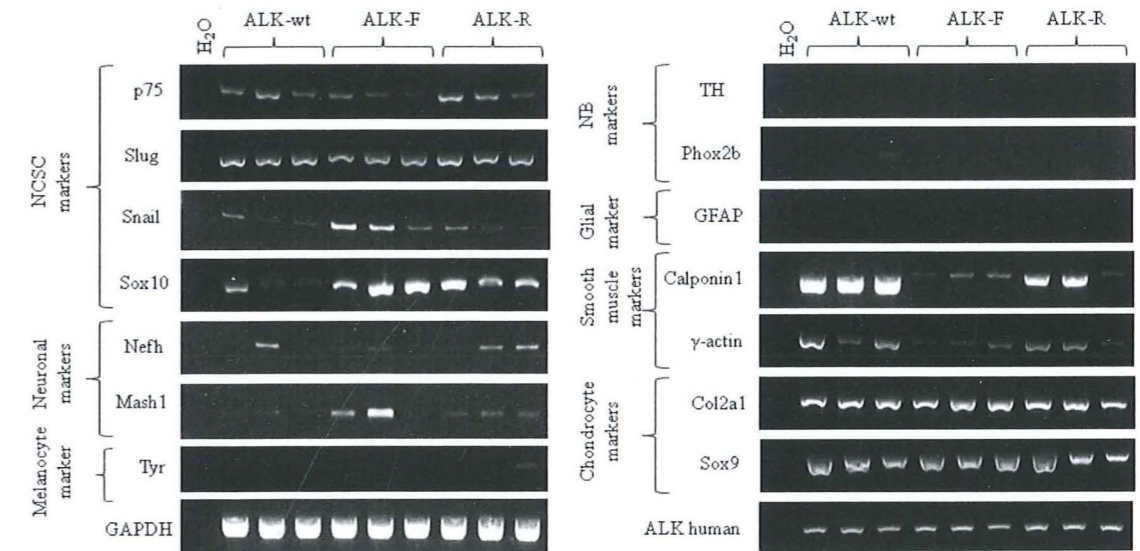


Figure 19: RT-PCR analysis of NCSC and differentiation markers in subcutaneous tumors. Three representative subcutaneous tumors for each transduced cell population (ALK-wt, ALK-F and ALK-R) were analyzed.

Subcutaneous tumors were also analyzed by histo-pathology. First, H&E labelling was performed to observe the tumor anatomy, cell morphology and whether NB-specific structures were noticed (Homer-Wright rosette). Then, IHC labelling was performed with different markers to identify the tumor type more precisely and exclude the several NB-like tumors, such as Ewing's sarcoma and melanoma. In H&E labeling (Figure 20), the tumors appeared as round or spindle-shaped blue cells. According to Dr Pu Yan (Institut Universitaire de Pathologie in Lausanne), all tumors of ALK-wt, ALK-F1174L, and ALK-R1245Q look like NB, with the same cell type and undifferentiated morphology, but should be correlated with IHC, and melanoma should be excluded. Histologically, no Homer-Wright rosettes were found, which are known to be pathognomonic for NB tumor.

Tumors	Markers						
	ALK	NCAM	CD44	NF	CD99	Tyr	Pax3
		Synapse, neural crest cells	Mesenchymal cells, favorable NB	Neurons	Ewing's sarcoma, T-cell lymphoma	Melanocytes	Melanocytes
ALK-wt	+++	-	+++	-	-	-	-
	+	+	+++	-	-	-	-
	++	++	+++	-	-	-	-
ALK-F	+	++	+++	-	-	-	-
	+	+	+++	-	-	-	-
	+	-	+++	-	-	-	-
ALK-R	+	+	+++	-	-	-	-
	++	+	+++	+/-	-	-	-
	+	+	+++	-	-	-	-

+ = slightly positive, ++ = positive, +++ = very positive, - = negative, +/- = mix of positive and negative zones

Table 6: Summary of H&E and IHC analyses in subcutaneous tumors. Three representative subcutaneous tumors for each transduced cell population (ALK-wt, ALK-F and ALK-R) were analyzed.

As summarized in Table 6 and illustrated in Figure 20, ALK and CD44 were found in all tumors. As tumors were driven by NCP transduced with mutated or wild-type ALK, ALK staining was expected. CD44 indicated mesenchymal cells or favorable NB in human. NCAM was present in most

tumors which was compatible with their neural crest origin. The absence of CD99, Tyr and Pax3 ruled out Ewing's sarcoma and melanoma, which resemble NB tumors.

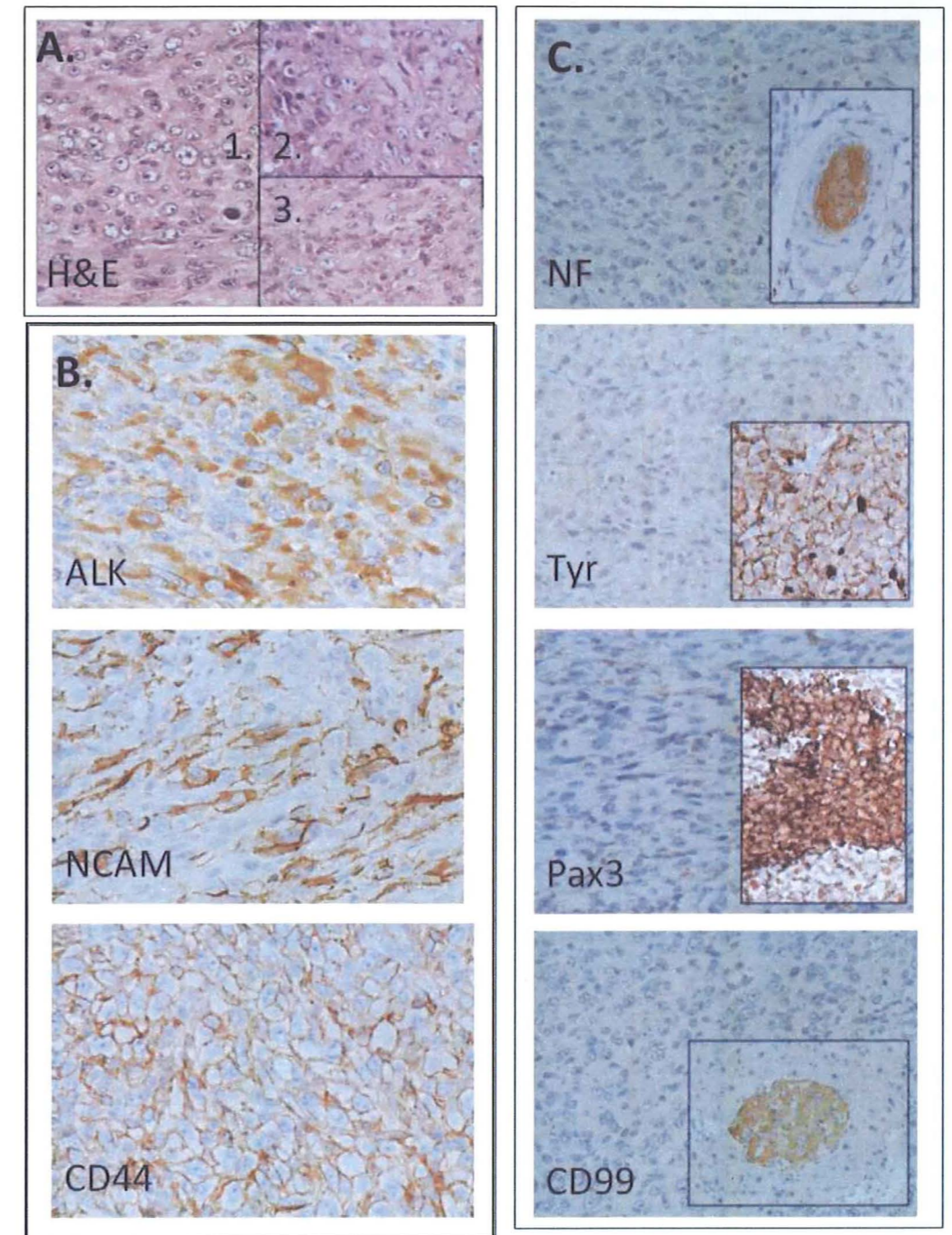


Figure 20: H&E and IHC stainings of representative subcutaneous tumors. (A.) H&E of one representative tumor of ALK-wt (1.), ALK-F1174L (2.), and ALK-R1245Q (3.) tumor groups. (B.) Positive markers found in subcutaneous tumors. (C.) Negative markers found in subcutaneous tumors with their positive controls.

Orthotopic implantations

Given the complexity of the interactions between tumor cells and their microenvironment, it was crucial to analyze the tumorigenicity of JoMa1 transduced cells in the orthotopic NB model, as the orthotopic model faithfully reproduces the tumor microenvironment. For negative controls, parental JoMa1 cells and JoMa1-Migr cells were used, as for subcutaneous injections. Tumor size was measured by ultrasonography during tumor growth, in absence of Tamoxifen.

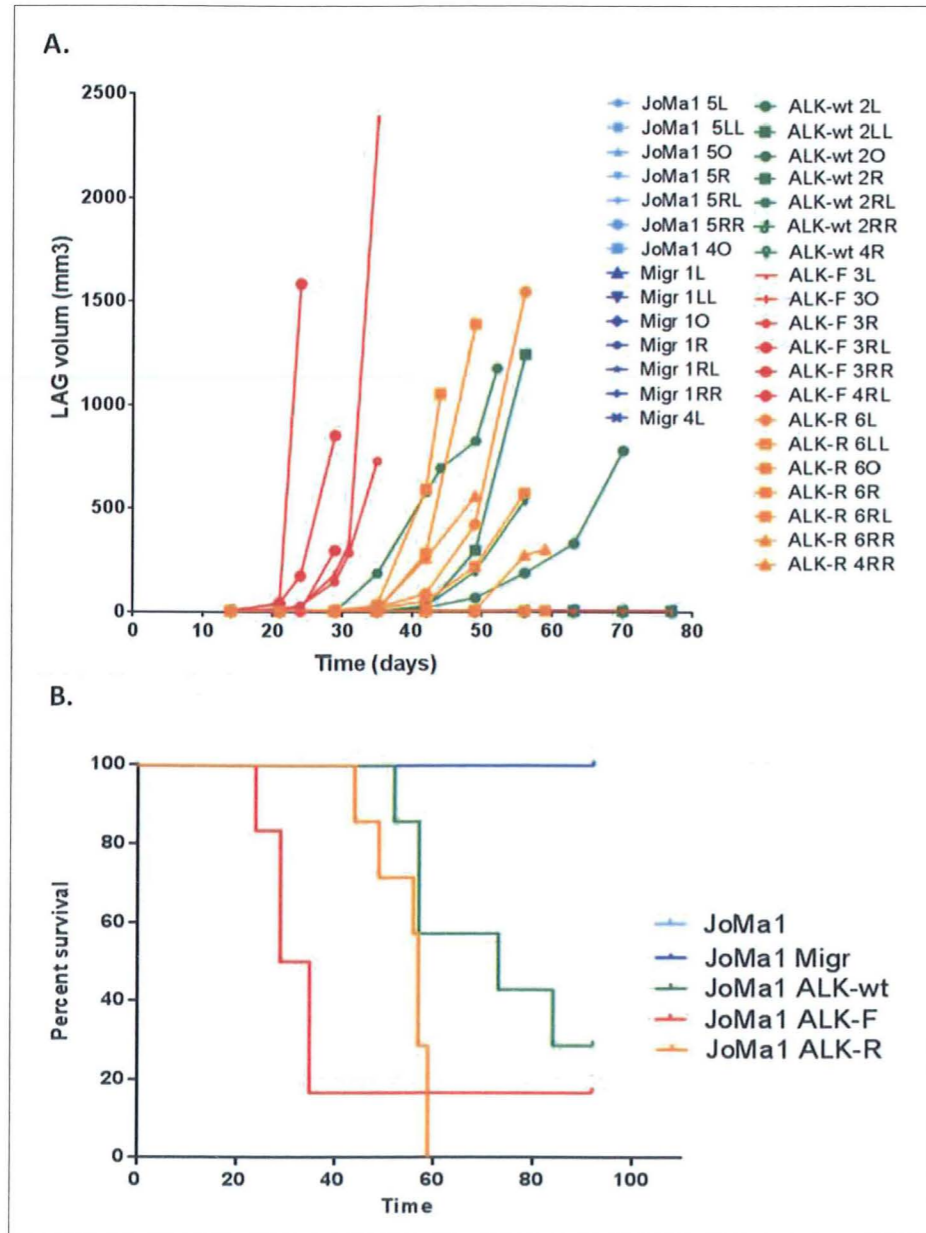


Figure 21: (A.) Growth of LAG tumor. The abdominal tumors are not represented. (B.) Kaplan-Meier survival curves

As shown in Figure 21, ALK-F1174L derived tumors grew the fastest with 5/6 affected mice. The ALK-F1174L mice had to be sacrificed between 24 and 35 days post-injection, except one which did not develop a tumor. All ALK-R1245Q mice were sacrificed between 45 and 59 days post-injection. Finally, ALK-wt-derived tumors grew the slowest with 5/7 mice affected, which were sacrificed from 52 to 84 days post-injection. All remaining mice were sacrificed 92 days post-injection. At dissection, one ALK-wt mouse presented a growing abdominal tumor, while no tumor was found in the last ALK-wt and ALK-F mice, and none in the negative controls.

Tumoral invasion in sacrificed mice is illustrated in Table 7. In ALK-F1174L group, out of 5 sacrificed mice, all presented adrenal tumors, one was associated with a big abdominal tumor, another had a small abdominal tumor and the three other mice had a probable metastasis on their spleen (not yet analyzed). In group ALK-R1245Q, out of 7 sacrificed mice, 6 mice presented an adrenal tumor of which 5 were associated with an abdominal tumor. The mouse with only an adrenal tumor died spontaneously without having its metastases analyzed. One ALK-R1245Q mouse had two immense abdominal tumors but no tumor in the adrenal gland. All abdominal tumors found in this group were just below the peritoneum and sometimes completely stuck to it. In the ALK-wt group, out of 6 sacrificed mice, 4 presented adrenal tumors and 2 only an abdominal tumor. With respect to dissemination, one mouse presented an enlarged, oedemateous, and potentially tumoral kidney (not yet analyzed) and another mouse had a possible metastasis on the spleen and an infiltrated kidney.

Group	Mouse	Day of sacrifice after orthotopic implantations	Adrenal tumor	Infiltrated kidney	Abdominal tumor	Others probable metastasis (not yet analyzed)
ALK-F	3-RL	24	1	-	1	-
	4-RL	29	1	-	-	Spleen
	3-RR	29	1	-	-	Spleen
	3-R	35	1	-	-	Spleen
	3-O	35	1	1	1	-
ALK-R	6-RL	45	1	-	1	-
	6-R	49	1	1	1	Spleen
	6-LL	57	1	1	1	-
	6-L	57	1	-	1	-
	4-RR	56	1	-	-	-
	6-O	59	-	-	2	Spleen, Stomach
	6-RR	59	1	-	1	-
ALK-wt	2-RL	52	1	-	-	-
	2-R	57	1	1	-	Spleen
	4-R	57	1	Oedemateous left kidney	-	-
	2-O	73	1	-	-	-
	2-L	84	-	-	2	-
	2-LL	92	-	-	1	-

Table 7: Day of sacrifice and description of tumoral invasion in orthotopically injected mice

Discussion

NB is known to originate from NCPC, and ALK was found to be mutated or amplified in a subset of NB. To analyze the role of ALK in the oncogenesis of NB, we introduced wild-type ALK and its most frequent mutations, F1174L and R1245Q, in the NCPC JoMa1 immortalized with an inducible c-MycER. First, some *in vitro* tests were performed to assay the c-MycER system of JoMa1 cells, the stability of transduced cells, their phenotypes, growth and transforming capacities. Then, we injected these cells subcutaneously in nude mice, and finally orthotopically in the adrenal gland to determine whether ALK wild-type or mutated genes were sufficient to drive neuroblastomagenesis from NCPC.

The first step was to test the c-MycER system of JoMa1 cells inducible by Tamoxifen. The c-MycER on/off switch was demonstrated by Western-Blot with the translocation of c-MycER in presence of Tamoxifen from cytoplasm to nucleus, where activated c-MycER is able to transactivate its target genes, while in absence of Tamoxifen c-MycER is inactivated in the cytoplasm. Then, the functional effect of the c-MycER system in JoMa1 cells was observed by growth assay with a highly increased cell proliferation resulting from c-MycER activation, compared to c-MycER inactivation, as reported in previous study [66]. Thus, the c-MycER on/off switch was highlighted at molecular and functional levels, which allowed us to rule out an effect of the proto-oncogene c-MycER in further *in vivo* tests performed without Tamoxifen.

After introduction of wild-type and mutated *ALK* genes in JoMa1 cells by retroviral infection, most transduced JoMa1 cells still expressed p75, which indicated that the transduction process did not differentiate JoMa1 cells, and that they kept their NCPC properties. Stable ALK RNA and protein expression were then confirmed in ALK-wt, ALK-F1174L, and ALK-R1245Q transduced cell lines.

As NCPC, transduced JoMa1 cells are expected to be in an undifferentiated state. In the original article, JoMa1 cells were positive for the NCPC markers p75, Slug, Sox10 and slightly for Snail, while differentiation markers Mash1, Nefh, γ -actin, Calponin, Tyr, and Col2a1 were not detected [54]. As observed by RT-PCR, our transduced JoMa1 cells expressed NCPC markers, but also smooth muscle and chondrocyte markers. However, that was not induced by transduction process as the parental JoMa1 cells also expressed these markers. Sox9 is highly expressed in JoMa1 cells, but according to other published reports the specificity of chondrocyte markers is controversial. In addition to Sox9 expression from prechondrocytic mesenchymal condensations to fully differentiated chondrocytes [67], it also possesses several roles in development (testes, pancreas, intestine, brain, kidney, heart valves and derivatives of neural crest) and diseases (carcinomas and fibrosis-related disorders), and more relevant for JoMa1 cells, Sox9 is required for formation and maintenance of neural stem cells in mouse embryogenesis and acts in specification of glial lineage [68]. Thus, Sox9 seems to be a non-

specific marker for chondrocyte differentiation. The Col2a1 (mouse type II collagen) marker is expressed in chondroprogenitor cells and in chondrocytes, but also in some areas of central nervous system, heart and other localizations [69]. Interestingly, ectopic expression of Sox9 was shown to induce ectopic expression of Col2a1 [69]. So the weak Col2a expression in JoMa1 cells may be induced by Sox9. Thus, these chondrocyte markers are not highly specific. Nevertheless, we cannot exclude that a part of JoMa1 cell population is initiating a smooth muscle differentiation, even in the presence of NCPC markers. Immunofluorescence or FACS analyses would be more adequate to determine the percentage of cells expressing differentiation markers.

The influence of the expression of wild-type or mutated ALK on the differentiation potential of NCPC definitely needs future analyses. Especially given the previous results of orthotopic injections of Monc1 cells (NCPC immortalized by constitutive v-Myc), which gave rise to 50% of tumors resembling chondrosarcome or osteosarcome, and 50% of NB-like tumors, while 100% of the tumors driven by ALK-F1174L Monc1 cells were NB-like. This could indicate a preference of the *ALK* gene to drive NB tumors, compared to the v-myc oncogene. A differentiation test of JoMa1 cells was indeed performed, and results were analyzed by RT-PCR. But RT-PCR seems to not be the best method of analysis. Immunofluorescence should have been carried out, but could not be performed due to lack of time.

The influence of c-MycER on/off switch and ALK mutations on endogenous c-Myc and MycN expressions was explored by a Real-Time PCR of their respective mRNA expression levels. The results showed that endogenous c-Myc mRNA was 2.5 times more abundant when c-MycER was activated by Tamoxifen, which confirmed a slight increase of endogenous c-Myc protein expression level observed by Western-Blot in presence of Tamoxifen. As the c-Myc primer used was mouse specific, human c-MycER should not be detected [70]. Thus, the activation of c-MycER induces a weak increase of endogenous c-Myc expression, which was not observed in original JoMa1's report where c-Myc amount was comparable with and without c-MycER activation [54]. In the absence of c-MycER activation, ALK-F1174L and ALK-R1245Q transduced cells expressed about 4 times more c-Myc mRNA than ALK-wt and untransduced JoMa1 cells, which suggests an effect of constitutively activated ALK on endogenous c-Myc mRNA expression level. These results are in accordance with a study from Raetz and al. [71] showing that c-Myc is expressed in 100% of NMP/ALK positive lymphoma, while c-Myc was not expressed in NMP/ALK negative lymphoma, suggesting that c-Myc may be a downstream target of ALK signaling. Therefore, endogenous c-Myc expression may be increased by ALK-F1174L- and ALK-R1245Q-activating mutations, as demonstrated by NMP/ALK-activating fusion mutation. Regarding MycN mRNA expression levels in transduced JoMa1 cells, it seems to be decreased when c-Myc is increased. It has been already shown in 1989 that when MycN and c-Myc are co-expressed, c-Myc predominates, but the lack of c-Myc amplification allows MycN

expression to increase [72]. Conversely, in MycN-amplified NB, c-Myc seems to be repressed by MycN [73]. Thus, in JoMa1 cells, where MycN is present but not amplified, higher levels of c-Myc induced by Tamoxifen or ALK mutants seem to decrease MycN expression, except in the JoMa1-ALK-F1174L cell line. However, it is possible that ALK-F1174L induces a stronger increased MycN expression, which counterbalances the decrease of MycN expression caused by c-Myc increase more efficiently than with ALK-R1245Q. At the RNA level, ALK activation was already shown to regulate MycN promoter activity by increasing MycN transcriptional initiation, which could be blocked by specific ALK inhibitors. This somewhat explains the cooperation between ALK-F1174L and amplified MycN [74]. At the protein level, ALK-F1174L was shown to stabilize MycN protein by stronger S⁶² phosphorylation via ERK signaling pathway, which is associated with a slightly elevated MycN protein level [58]. Another possible cause is that combined activation increase of PI3K/AKT and RAS/ERK pathways by ALK stabilizes MycN in tumors co-expressing ALK-F1174L and MycN [75]. And indeed, AKT and ERK were shown to be more phosphorylated in transduced ALK-F1174L JoMa1 cells than in the ALK-R1245Q JoMa1 cell line (Figure 11). It would therefore be interesting to assess the MycN protein level in JoMa1 transduced cells to check whether it is higher in ALK-F1174L cell line.

Activation by phosphorylation of three ALK-signaling pathways JAK/STAT3, PI3K/AKT, and RAS/MAPK was analyzed by phospho-Western-Blot. Phosphorylated ALK, which indicates ALK activation, was present in ALK-F1174L and ALK-R1245Q JoMa1 cell lines, and weakly in ALK-wt JoMa1 cells. This confirms that ALK-F1174L and ALK-R1245Q mutations induce a constitutive activation of ALK in these NCP. According to De Brouwer's study [28], ALK-F1174L induces a higher level of ALK phosphorylation than ALK-R1245Q, which was not confirmed by our phospho-Western-Blot. ALK 140 kD isoform was weakly phosphorylated in ALK-wt JoMa1 cell line. A low activation of ALK protein by phosphorylation was already described in NB cell lines expressing ALK-wt [28]. Moreover, Passoni and al. reported that 140 kD isoform was constitutively phosphorylated in highly ALK-wt expressing cells, suggesting the existence of a critical threshold for oncogenic activation [29]. Thus, ALK-wt JoMa1 cell line could express a sufficient level of ALK-wt proteins for auto-activation by phosphorylation. Surprisingly, the truncated ALK 140 kD isoform was more phosphorylated than the 220 kD isoform in wild-type as well as in mutated ALK cell lines and the phosphorylated 220 kD isoform was not detected in cell lines cultured in absence of Tamoxifen. The development of tumors without Tamoxifen suggests that the 140 kD isoform may be more essential for oncogenic activity than 220 kD isoform. It would be interesting to perform phospho-Western-Blot on obtained tumors and compare the respective amount of phosphorylated ALK isoforms. However, in NB cell lines, the two isoforms were already found to be phosphorylated [29, 74].

An increase in activation of the three ALK signaling pathways was expected with mutated ALK, as ALK is constitutively activated. Nevertheless, AKT pathways were slightly more activated in both mutated ALK cell lines with Tamoxifen and in ALK-F1174L JoMa1 cells without Tamoxifen. The ERK pathway was clearly more activated with ALK-F1174L, which may allow MycN stabilization, as previously mentioned. These observations contradict a previous study showing that ALK-F1174L phosphorylated STAT3 and AKT, while ALK-R1245Q phosphorylated ERK1/2 and AKT in IL-3 deprived Ba/F3 cells [48]. This discrepancy may be due to a species difference. However, Berry and al. [75] described that ALK-F1174L activated PI3K/AKT and RAS/ERK pathways leading to an increased survival in mice, which seems to be also the case in the present study. Surprisingly, a basal activation of the three signaling pathways activated by phosphorylated ALK was observed in all cell lines independently of ALK activation, suggesting that these pathways may be activated by others RTKs. It is difficult to highlight the signaling pathways activated by only one RTK such as ALK, because negative or positive feedbacks can modify the response in the RTK signaling network [76], just as the crosstalk between various RTKs can affect signaling pathways after ALK activation [77]. To decrease RTK activation by growth factors, cells were starved with 2.5% JoMa1 medium, but the basal activation of these signaling pathways was not reduced (data not shown). Therefore the activation of signaling pathways by ALK cannot be clearly distinguished from activation by other RTKs.

In the *in vitro* assays performed to assess the growth capacity of the transduced JoMa1 cells, the 2D culture (growth assay) was less conclusive to distinguish wild-type and mutated *ALK* genes effect than 3D culture (sphere and methylcellulose assays). But surprisingly, growth assays in unfavorable conditions (25% of JoMa1 medium) resulted in higher proliferation rates than in 100% JoMa1 medium. This suggests that parental JoMa1 cells proliferate better under stress conditions and that this reaction capacity was not affected by transduction of wild-type and mutated ALK. Alternatively, one or several factors in the JoMa1 medium may act negatively to cell proliferation when present in high concentration.

In sphere assays, when c-MycER was inactive, JoMa1 cells were unable to self-renew or proliferate more than 2 or 3 passages, while ALK-F1174L produced spheres up to 5 passages and ALK-R1245Q JoMa1 cells up to 4 passages. ALK-F1174L transduced in JoMa1 cells by Schulte and al. [3] showed also a maintained proliferation capacity in absence of Tamoxifen. In addition, in two studies, these mutations were transduced in Ba/F3 cells. The first study showed a growth independent for IL-3, and faster growth for ALK-F1174L than ALK-R1245Q [28]. The second showed a better cell proliferation in IL-3 reduced concentration for cells expressing F1174L and R1245Q mutation than ALK-wt or ALK-T1151M. And without IL-3, only F1174L or R1245Q mutants survived [48]. Their resistance capacity may be explained in part by the anti-apoptotic effect of intrinsically activated ALK [45].

Moreover, sphere forming capacities increased at each passage in presence of active c-MycER and in particular for ALK-F1174L and ALK-R1245Q JoMa1 cell lines. This can be explained by the selection of cells having higher proliferation capacity thanks to ALK constitutive activation.

A tumorigenic assay in methylcellulose was performed as a representative assay of future *in vivo* tests. With ALK-F1174L and ALK-R1245Q cell lines, we observed an increased number of large colonies with c-MycER activation, while in the absence of c-MycER activation the difference with control cells was not significant. The c-MycER activity may be required to stimulate 3D growth in this semi-solid medium, and ALK mutations are not able to compensate the absence of c-MycER. Despite that, constitutive activation of ALK in JoMa1 cells seems to give an advantage in 3D growth. This is in accordance with a previous study showing that NIH3T3 transfected with ALK-F1174L, K1062M, and the protein fusion EML4-ALK also displayed an increase in colony formation in soft agar compared to ALK-wt [30].

A first *in vivo* assay was performed by subcutaneous implantations of ALK-wt, ALK mutants (F1174L and R1245Q) and controls (parental JoMa1 and JoMa1 cells transduced with vector pMigr) in nude mice. Mice injected with ALK-F1174L JoMa1 cells were the first to present tumors followed by ALK-R1245Q and then ALK-wt groups. That was not surprising, as ALK-F1174 had already been indicated to display a higher transforming capacity compared to ALK-R1245Q [28, 74, 78]. 100% tumor take was observed in ALK-F1174L and ALK-R1245Q groups as 6/6 injected sites developed tumors, compared to 4/6 for ALK-wt group. Interestingly, ALK-wt displayed a tumorigenic capacity *in vivo*, even if weaker than ALK mutants, despite the fact that *in vitro* in methylcellulose assay, ALK-wt did not show increased tumorigenic ability compared to controls. The tumorigenic capacity of ALK mutants *in vivo* was already explored by Schulte and al. [3] who also injected subcutaneously JoMa1 cells transfected with ALK-F1174L in nude mice, but they obtained tumor formation in only 2/6 mice. Chen and al. [30] transfected NIH3T3 fibroblasts with wild-type ALK and mutants (F1174L, K1062M and EML4-ALK), which were then injected subcutaneously in nude mice. They obtained 100% of tumorigenesis with mutants but nothing with wild-type ALK. However, an oncogenic effect of ALK-wt had already been reported by Passoni and al. [29] with an ALK constitutive activation and an aberrant ALK phosphorylation in IMR-32 cells, an NB cell line expressing ALK-wt. They also demonstrated that inhibition of ALK in NB cells overexpressing wild-type or mutated ALK induced growth arrest and cell death. In addition, a greater proportion of ALK overexpressing NB was shown to be present in unfavorable stages than in localized stages. They concluded that ALK-wt possess a threshold of expression to achieve an oncogenic effect and that other mechanisms than mutation or amplification regulate ALK expression level. Thus, incomplete tumorigenic capacity of ALK-wt in our subcutaneous assays can be explained by ALK-wt expression variation, with a threshold of expression needed to achieve tumorigenicity that was not systematically attained. In the future it

would be interesting to analyze ALK activation level in ALK-wt derived tumors to determine whether they increased constitutive activation during tumorigenesis. The negative controls JoMa1 and JoMa1-Migr did not present any tumors, which ruled out an influence of the pMigr vector in tumorigenesis, or a role of c-mycER. Most importantly, as tumors grew only in wild-type and mutated ALK groups, the ALK expression in NCPC seems to play an essential role in tumor initiation.

The next step was to characterize these tumors. Thus, RT-PCR and immunohistochemistry were performed on subcutaneous tumors of wild-type and mutated ALK groups to distinguish JoMa1 cells proliferation from NB or other tumor type formation. As observed by RT-PCR, all tumors expressed NCSC markers, but also smooth muscle and chondrocyte markers, which was not surprising as transduced JoMa1 cells were already expressing these markers before subcutaneous injections. P75, used here as an NCSC marker, was described to be present in differentiated NB and absent in poorly differentiated NB [79]. The other NCSC marker, Slug, was also detected in NB cell lines [80]. Concerning smooth muscle markers, requiring vessels to feed cells, tumors may contain some arterioles or venules containing smooth muscle. Most tumors expressed neuronal markers, which did not exclude NB tumor type, because Mash1 was shown to be highly expressed in NB [81], tumors can be innervated and NB is a neuro-endocrine tumor. One ALK-R1245Q tumor was positive for the melanocyte marker, which can be due to a subcutaneous cell environment possibly promoting this means of differentiation or perhaps some subcutaneous cells were also removed during dissection. Only one ALK-wt tumor expressed Phox2b, an NB marker. Phox2b plays an important role in the differentiation of autonomic neurons [82], and is expressed in some cells of the autonomic nervous system as neurons of sympathetic ganglia or chromaffin cells of adrenal medulla [83]. In addition Phox2b mRNA was shown to be nearly always elevated in neuroblastic tumors and to be a highly sensitive and specific NB marker by IHC in pediatric small round blue-cell tumors [83].

The histo-pathology of subcutaneous tumors was compatible with NB-like tumors in cell type and morphology. The others NB-like tumors, such as melanoma and Ewing's sarcoma, were ruled out by IHC markers. Nevertheless, these results need to be completed with NB markers, such as TH or Synaptophysin, but the specificity of NB markers appears to be different in mice and humans. For example, the presence of CD44 in human NB was shown to be a good prognostic factor [84]. But interestingly, Valentiner and al. reported that expression of CD44 in human NB cells injected subcutaneously in mice was associated with metastatic pattern [85], suggesting an opposite prognostic value of CD44 in mice and humans. Although the specificity of these markers in mice is debatable, we don't possess a lot of tools to characterize NB. Thus, even if RT-PCR did not allow a clear tumor characterization, except for one wild-type tumor expressing Phox2b, NB tumor type was not excluded. Histology leans towards for NB tumor and analyses should be completed with other NB markers.

Transduced JoMa1 cells were orthotopically implanted into the adrenal gland of nude mice. This orthotopic NB model was demonstrated to faithfully reproduce the clinical appearance of human NB [62]. Indeed, orthotopic implantation of cells allows interaction with the microenvironment, which is known to play an important role in regulation of stem cell fate [86] and in tumorigenesis by interaction of microenvironment with tumor stem cells [87]. So it was important to analyze the tumorigenic capacity of ALK-wt and mutants in the natural NB microenvironment. Orthotopic injections confirmed the growth results obtained in subcutaneous injections. Indeed, mice injected with ALK-F1174L JoMa1 cells already presented tumors after 24 days and needed to be sacrificed early followed by mice bearing ALK-R1245Q and ALK-wt JoMa1 cells. Tumor take was incomplete for ALK-wt group, as previously observed in subcutaneous injection. The main differences between subcutaneous and orthotopic injections were that in orthotopic groups, tumors appeared in several different sites (adrenal gland, abdomen, spleen, kidney, and stomach) and the tumor take of ALK-F1174L group was not 100% in orthotopic conditions as 1/6 mice did not develop any tumors. Surprisingly, dissemination sites (kidney, spleen, abdomen, and stomach) were not typical anatomic sites for NB metastasis and some mice developed only abdominal tumors. In the orthotopic NB model developed by Joseph and al. [62], mice did not present tumors in sites other than bone marrow and liver, which are sites of human NB metastasis due to hematologic dissemination [62]. However, in transgenic mice co-expressing ALK-F1174L and MycN, Berry and al. [75] also obtained abnormal dissemination sites (“thoracic and abdominal masses that arose in the paraspinal ganglia and adrenals” but also “focal masses on the forelimb, neck and shoulder”). Thus, in future analyses, it will be interesting to assay whether abdominal and adrenal tumors are both NB-like tumors. If NCPC transduced with wild-type or mutated ALK are able to induce NB formation in the abdominal cavity, this would suggest that microenvironment is not essential in NB differentiation and that the *ALK* gene can be sufficient for NB tumorigenesis, regardless of anatomic localization. In addition, the NB metastasis development in our mice may be in part impaired by fast tumoral growth.

In 2012, while this study was ongoing, two reports were published on ALK-F1174L and MycN implication in NB initiation, both using transgenic mice [58, 75]. In Heukamp’s study [58], mice expressing ALK-F1174L in neural crest derivatives were created. Among these transgenic mice, 5/12 mice developed tumors in retroperitoneal or neck regions between 130 and 351 days of age. Two mice also presented hepatic metastasis, and another a mediastinal lesion. They explained the incomplete penetrance and the relatively long time frame required for tumor development by the necessity of a second genetic event to occur. Indeed, chromosomal aberrations were observed in these tumors, that corresponded syntenically to the aberrations usually found in human NB (q1 gain, 17 gain, MycN amplification). But in tumors from mice expressing both ALK-F1174L and MycN by transgenic process, chromosomal aberrations were reduced, as if both abnormalities were sufficient to drive NB initiation. That can be explained by the two-hit hypothesis of Alfred G. Knudson, where two mutations

are generally necessary to induce a tumor [88]. MycN overexpression and ALK mutation are two possible hits able to drive NB tumor genesis. Given these results it would be interesting to analyse if our tumors express other chromosomal aberrations. In Berry’s study [75], transgenic mice expressing ALK-F1174L and ALK-wt in neural crest cells did not develop tumor. But all transgenic mice co-expressing ALK-F1174L and MycN amplification had to be sacrificed due to tumor growth. These two studies demonstrated the synergy between ALK-F1174L and MycN amplification for driving NB, but only Heukamp’s study showed the capacity of ALK-F1174L to drive neuroblastomagenesis alone. The discrepancy between these two studies may be due to the different expression levels of ALK in transgenic mice, as different promoters were used to drive ALK expression in each transgenic model. The ability of ALK-wt to drive tumorigenicity in our JoMa1 cells may be due to its high expression level, which may be sufficient for its constitutive activation, as previously discussed.

Therefore, our study brings additional results confirming the ALK-F1174L tumorigenic capacity from NCPC in an orthotopic model, and demonstrates for the first time that ALK-wt and ALK-R1245Q are also able to drive NB initiation from NCPC. Moreover, tumors grew in absence of Tamoxifen which rules out the participation of c-MycER activation in tumorigenesis.

Conclusion and perspectives

ALK mutations, amplification and overexpression have been described in a subset of NB. As already shown in previous studies, we confirm that ALK-F1174L has a stronger tumorigenic capacity than ALK-R1245Q, and that both express ALK constitutive activation and possess tumorigenic properties *in vitro*. *In vivo*, we demonstrated that expression of ALK-F1174L is sufficient to induce tumor formation from neural crest progenitor cells in an orthotopic model of NB, and for the first time that ALK-wt or ALK-R1245Q are also able to induce tumorigenesis.

The next step of the project will be to analyze obtained orthotopic tumor types to confirm that wild-type and mutated ALK drive neuroblastomagenesis from NCPC. Given the difficulty of classifying tumor type in subcutaneous tumors, we intend to perform transcriptomic profiling of orthotopic tumors, and to compare results using the NB-specific database of the Curie Institut of Paris. Tumor histology will also be analyzed for NB markers using H&E and IHC. With the results of transcriptomic profiles, others genomic expression aberrations can be identified allowing to highlight a possible second hit in tumorigenesis or deregulation of gene expression important for tumorigenicity. In addition, difference in gene expression profiles between the orthotopic tumors derived from JoMa1-ALK-wt, -ALK-F, or -ALK-R cells may be identified through this analysis.

Orthotopic tumors were dissociated and tumoral JoMa1 cells were cultured *in vitro* to determine whether tumoral transformation results in new properties. Indeed, ALK inhibitor resistance could be assayed on these cells to test whether they are sensitive to this therapy or if they acquired independence from ALK oncogenic activity.

It will be also interesting to analyze ALK expression and activation by phospho-Western-Blot in tumors, as a potential correlation between constitutive activation and high ALK expression had been reported by Passoni and al. [29] in ALK-wt tumors. Moreover the phosphorylated state of ALK isoforms could indicate whether one of them is more important for tumorigenesis. Also, the analyses of signaling pathways activation in all tumor groups could indicate whether a pathway is essential for tumor growth or if the activation profile is different in tumors driven by ALK-F1174L, ALK-R1245Q, or ALK-wt. Regarding RTK expression, as ALK signaling pathways are probably also activated by other RTKs and a crosstalk between different RTKs was described in cancer [77], perhaps a putative correlation between ALK and Trk should be studied.

Given our dissemination sites in the orthotopic model, it could be interesting to inject fewer cells in the adrenal gland in future orthotopic experiments to allow more time for metastatic dissemination, or to inject cells in blood circulation to highlight a possible chemotropism of NCPC for sympathetic

nervous system tissues or others sites. In addition, ALK inhibitor use on mice presenting adrenal tumors after orthotopic injection would allow confirmation of the importance of ALK expression in tumorigenesis. Orthotopic implantation with mice treated with Tamoxifen could also highlight a potential cooperation of c-Myc and ALK in tumorigenesis.

Acknowledgements

First and foremost, I thank the Dr Nicole Gross for giving to me the opportunity to work in her laboratory and for having supervised my thesis with her communicative dynamism, her long experience in research and the benefit of her scientific relations.

It was also a pleasure to be supervised by Dr Annick Müllenthaler-Mottet, who coached me very closely with kindness and taught me a lot of scientific concepts and how to manage the work involved in writing a doctoral thesis. Katia Bourloud-Balmas passed down her long practical experience in cell culture and bio-chemical manipulations, always with a smile and good mood. In addition, Annick and Katia supported me very often in helping me to take care of my very demanding cells.

Dr Jean-Marc Joseph and Dr Nicolas Jauquier performed the orthotopic injections with their impressive surgical abilities. With Nicolas, I also shared the questions and thoughts of physicians beginning their work in a research laboratory, and did so with great pleasure.

Dr Marjorie Flahaut-Chételat, Katya Nardou-Auderset, Dolorès Mosig and Dr Julie Lieberman answered all my questions with enthusiasm and kindness, were joyful co-workers and provided support during my doubts and worries.

Dr Emma Garcia answered my clinical questions with her sunny dynamism and I discovered with fascination her very important and demanding work for children in Swiss and international oncological networks.

Alexandre Sarre from CAF – Cardiovascular Assessment Facility – took the time to perform all the echographies of orthotopically injected mice with patience and efficiency. Jean-Christophe Stehle from the Mouse Pathology of Lausanne did all immunohistochemical analyses on mouse tissues and Dr Pu Yan from Pediatric Pathology of Lausanne gave me her professional interpretation of these immunohistochemical analyses.

And last but not least, David Sulc supported me mentally the whole year during and corrected my English text with his attention to detail and subtle language knowledge.

With all of you who were present in the research laboratory, I spent very friendly and sometimes funny coffee breaks (which could also be called “chocolate breaks” given our shared passion ;-)).

I thank each and every one of you for this wonderful year... I will miss you! And I hope we will keep in touch!

References

1. Le Douarin, N.M., G.W. Calloni, and E. Dupin, *The stem cells of the neural crest*. Cell Cycle, 2008. **7**(8): p. 1013-9.
2. Le Douarin, N.M., et al., *Neural crest cell plasticity and its limits*. Development, 2004. **131**(19): p. 4637-50.
3. Schulte, J.H., et al., *MYCN and ALKF1174L are sufficient to drive neuroblastoma development from neural crest progenitor cells*. Oncogene, 2013. **32**(8): p. 1059-65.
4. Hoehner, J.C., et al., *A developmental model of neuroblastoma: differentiating stroma-poor tumors' progress along an extra-adrenal chromaffin lineage*. Lab Invest, 1996. **75**(5): p. 659-675.
5. Knecht, A.K. and M. Bronner-Fraser, *Induction of the neural crest: a multigene process*. Nat Rev Genet, 2002. **3**(6): p. 453-61.
6. Wright, J.H., *Neurocytoma or Neuroblastoma, a Kind of Tumor Not Generally Recognized*. J Exp Med, 1910. **12**(4): p. 556-61.
7. Maris, J.M., et al., *Neuroblastoma*. Lancet, 2007. **369**(9579): p. 2106-2120.
8. Acharya, S., et al., *Prenatally diagnosed neuroblastoma*. Cancer, 1997. **80**(2): p. 304-10.
9. London, W.B., et al., *Evidence for an age cutoff greater than 365 days for neuroblastoma risk group stratification in the Children's Oncology Group*. J Clin Oncol, 2005. **23**(27): p. 6459-65.
10. Brodeur, G.M., *Neuroblastoma: biological insights into a clinical enigma*. Nat.Rev.Cancer, 2003. **3**(3): p. 203-216.
11. DuBois, S.G., et al., *Metastatic sites in stage IV and IVS neuroblastoma correlate with age, tumor biology, and survival*. J Pediatr Hematol Oncol, 1999. **21**(3): p. 181-9.
12. Colon, N.C. and D.H. Chung, *Neuroblastoma*. Adv Pediatr, 2011. **58**(1): p. 297-311.
13. Sharp, S.E., M.J. Gelfand, and B.L. Shulkin, *Pediatrics: diagnosis of neuroblastoma*. Semin Nucl Med, 2011. **41**(5): p. 345-53.
14. Brodeur, G.M., et al., *Revisions of the international criteria for neuroblastoma diagnosis, staging, and response to treatment [see comments]*. J.Clin.Oncol., 1993. **11**(8): p. 1466-1477.
15. Janoueix-Lerosey, I., G. Schleiermacher, and O. Delattre, *Molecular pathogenesis of peripheral neuroblastic tumors*. Oncogene, 2010. **29**(11): p. 1566-79.
16. Pugh, T.J., et al., *The genetic landscape of high-risk neuroblastoma*. Nat Genet, 2013. **45**(3): p. 279-84.
17. Janoueix-Lerosey, I., et al., *Somatic and germline activating mutations of the ALK kinase receptor in neuroblastoma*. Nature, 2008. **455**(7215): p. 967-70.
18. Cohn, S.L., et al., *The International Neuroblastoma Risk Group (INRG) classification system: an INRG Task Force report*. J Clin Oncol, 2009. **27**(2): p. 289-97.
19. Maris, J.M., *Recent advances in neuroblastoma*. N Engl J Med, 2010. **362**(23): p. 2202-11.
20. Seeger, R.C., et al., *Association of multiple copies of the N-myc oncogene with rapid progression of neuroblastomas*. N.Engl.J.Med., 1985. **313**(18): p. 1111-1116.
21. Weiss, W.A., et al., *Targeted expression of MYCN causes neuroblastoma in transgenic mice*. EMBO J., 1997. **16**(11): p. 2985-2995.
22. Prochownik, E.V. and P.K. Vogt, *Therapeutic Targeting of Myc*. Genes Cancer, 2010. **1**(6): p. 650-659.
23. Matthay, K.K., R.E. George, and A.L. Yu, *Promising therapeutic targets in neuroblastoma*. Clin Cancer Res, 2012. **18**(10): p. 2740-53.
24. Morris, S.W., et al., *Fusion of a kinase gene, ALK, to a nucleolar protein gene, NPM, in non-Hodgkin's lymphoma*. Science, 1994. **263**(5151): p. 1281-4.
25. Chiarle, R., et al., *The anaplastic lymphoma kinase in the pathogenesis of cancer*. Nat Rev Cancer, 2008. **8**(1): p. 11-23.
26. Griffin, C.A., et al., *Recurrent involvement of 2p23 in inflammatory myofibroblastic tumors*. Cancer Res, 1999. **59**(12): p. 2776-80.

27. Lamant, L., et al., *Expression of the ALK tyrosine kinase gene in neuroblastoma*. Am J Pathol, 2000. **156**(5): p. 1711-1721.
28. De Brouwer, S., et al., *Meta-analysis of neuroblastomas reveals a skewed ALK mutation spectrum in tumors with MYCN amplification*. Clin Cancer Res, 2010. **16**(17): p. 4353-62.
29. Passoni, L., et al., *Mutation-independent anaplastic lymphoma kinase overexpression in poor prognosis neuroblastoma patients*. Cancer Res, 2009. **69**(18): p. 7338-46.
30. Chen, Y., et al., *Oncogenic mutations of ALK kinase in neuroblastoma*. Nature, 2008. **455**(7215): p. 971-4.
31. Mosse, Y.P., et al., *Identification of ALK as a major familial neuroblastoma predisposition gene*. Nature, 2008. **455**(7215): p. 930-5.
32. Ogawa, S., et al., *Oncogenic mutations of ALK in neuroblastoma*. Cancer Sci, 2011. **102**(2): p. 302-308.
33. Mathew, P., et al., *Localization of the murine homolog of the anaplastic lymphoma kinase (ALK) gene on mouse chromosome 17*. Cytogenet Cell Genet, 1995. **70**(1-2): p. 143-4.
34. Webb, T.R., et al., *Anaplastic lymphoma kinase: role in cancer pathogenesis and small-molecule inhibitor development for therapy*. Expert Rev Anticancer Ther, 2009. **9**(3): p. 331-56.
35. Azarova, A.M., G. Gautam, and R.E. George, *Emerging importance of ALK in neuroblastoma*. Semin Cancer Biol, 2011. **21**(4): p. 267-75.
36. Stoica, G.E., et al., *Identification of anaplastic lymphoma kinase as a receptor for the growth factor pleiotrophin*. J Biol Chem, 2001. **276**(20): p. 16772-16779.
37. Stoica, G.E., et al., *Midkine binds to anaplastic lymphoma kinase (ALK) and acts as a growth factor for different cell types*. J Biol Chem, 2002. **277**(39): p. 35990-35998.
38. Souttou, B., et al., *Activation of anaplastic lymphoma kinase receptor tyrosine kinase induces neuronal differentiation through the mitogen-activated protein kinase pathway*. J Biol Chem, 2001. **276**(12): p. 9526-31.
39. Zamo, A., et al., *Anaplastic lymphoma kinase (ALK) activates Stat3 and protects hematopoietic cells from cell death*. Oncogene, 2002. **21**(7): p. 1038-47.
40. Powers, C., et al., *Pleiotrophin signaling through anaplastic lymphoma kinase is rate-limiting for glioblastoma growth*. J Biol Chem, 2002. **277**(16): p. 14153-8.
41. Piccinini, G., et al., *A ligand-inducible epidermal growth factor receptor/anaplastic lymphoma kinase chimera promotes mitogenesis and transforming properties in 3T3 cells*. J Biol Chem, 2002. **277**(25): p. 22231-9.
42. Iwahara, T., et al., *Molecular characterization of ALK, a receptor tyrosine kinase expressed specifically in the nervous system*. Oncogene, 1997. **14**(4): p. 439-449.
43. Pulford, K., et al., *Detection of anaplastic lymphoma kinase (ALK) and nucleolar protein nucleophosmin (NPM)-ALK proteins in normal and neoplastic cells with the monoclonal antibody ALK1*. Blood, 1997. **89**(4): p. 1394-404.
44. Bilsland, J.G., et al., *Behavioral and neurochemical alterations in mice deficient in anaplastic lymphoma kinase suggest therapeutic potential for psychiatric indications*. Neuropsychopharmacology, 2008. **33**(3): p. 685-700.
45. Mourali, J., et al., *Anaplastic lymphoma kinase is a dependence receptor whose proapoptotic functions are activated by caspase cleavage*. Mol Cell Biol, 2006. **26**(16): p. 6209-22.
46. Bowden, E.T., G.E. Stoica, and A. Wellstein, *Anti-apoptotic signaling of pleiotrophin through its receptor, anaplastic lymphoma kinase*. J Biol Chem, 2002. **277**(39): p. 35862-35868.
47. Bourdeaut, F., et al., *ALK germline mutations in patients with neuroblastoma: a rare and weakly penetrant syndrome*. Eur J Hum Genet, 2012. **20**(3): p. 291-7.
48. George, R.E., et al., *Activating mutations in ALK provide a therapeutic target in neuroblastoma*. Nature, 2008. **455**(7215): p. 975-8.
49. Chand, D., et al., *Cell and Drosophila model systems define three classes of ALK mutations in neuroblastoma*. Dis Model Mech, 2012.
50. Mano, H., *ALKoma: A Cancer Subtype with a Shared Target*. Cancer Discov, 2012. **2**(6): p. 495-502.
51. Smith, K. and S. Dalton, *Myc transcription factors: key regulators behind establishment and maintenance of pluripotency*. Regen Med, 2010. **5**(6): p. 947-59.
52. Laurenti, E., A. Wilson, and A. Trumpp, *Myc's other life: stem cells and beyond*. Curr Opin Cell Biol, 2009. **21**(6): p. 844-54.
53. Rao, M.S. and D.J. Anderson, *Immortalization and controlled in vitro differentiation of murine multipotent neural crest stem cells*. J Neurobiol, 1997. **32**(7): p. 722-746.
54. Maurer, J., et al., *Establishment and controlled differentiation of neural crest stem cell lines using conditional transgenesis*. Differentiation, 2007. **75**(7): p. 580-591.
55. Osajima-Hakomori, Y., et al., *Biological role of anaplastic lymphoma kinase in neuroblastoma*. Am J Pathol, 2005. **167**(1): p. 213-222.
56. Stock, C., et al., *Genes proximal and distal to MYCN are highly expressed in human neuroblastoma as visualized by comparative expressed sequence hybridization*. Am J Pathol, 2008. **172**(1): p. 203-14.
57. Christensen, J.G., et al., *Cytoreductive antitumor activity of PF-2341066, a novel inhibitor of anaplastic lymphoma kinase and c-Met, in experimental models of anaplastic large-cell lymphoma*. Mol Cancer Ther, 2007. **6**(12 Pt 1): p. 3314-22.
58. Heukamp, L.C., et al., *Targeted Expression of Mutated ALK Induces Neuroblastoma in Transgenic Mice*. Sci Transl Med, 2012. **4**(141): p. 141ra91.
59. Stemple, D.L. and D.J. Anderson, *Isolation of a stem cell for neurons and glia from the mammalian neural crest*. Cell, 1992. **71**(6): p. 973-985.
60. Fuchs, S., et al., *Stage-specific control of neural crest stem cell proliferation by the small rho GTPases Cdc42 and Rac1*. Cell Stem Cell, 2009. **4**(3): p. 236-247.
61. Eliason, J.F., et al., *Non-linearity of colony formation by human tumour cells from biopsy samples*. Br J Cancer, 1985. **52**(3): p. 311-8.
62. Joseph, J.M., et al., *In vivo echographic evidence of tumoral vascularization and microenvironment interactions in metastatic orthotopic human neuroblastoma xenografts*. Int.J.Cancer, 2005. **113**(6): p. 881-890.
63. Paratore, C., et al., *Survival and glial fate acquisition of neural crest cells are regulated by an interplay between the transcription factor Sox10 and extrinsic combinatorial signaling*. Development, 2001. **128**(20): p. 3949-61.
64. Stemple, D.L. and D.J. Anderson, *Isolation of a stem cell for neurons and glia from the mammalian neural crest*. Cell, 1992. **71**(6): p. 973-85.
65. Jiang, X., et al., *Isolation and characterization of neural crest stem cells derived from in vitro-differentiated human embryonic stem cells*. Stem Cells Dev, 2009. **18**(7): p. 1059-70.
66. Jager, R., et al., *Cell type-specific conditional regulation of the c-myc proto-oncogene by combining Cre/loxP recombination and tamoxifen-mediated activation*. Genesis, 2004. **38**(3): p. 145-50.
67. Lefebvre, V. and B. de Crombrughe, *Toward understanding SOX9 function in chondrocyte differentiation*. Matrix Biol, 1998. **16**(9): p. 529-40.
68. Pritchett, J., et al., *Understanding the role of SOX9 in acquired diseases: lessons from development*. Trends Mol Med, 2011. **17**(3): p. 166-74.
69. de Crombrughe, B., et al., *Transcriptional mechanisms of chondrocyte differentiation*. Matrix Biol, 2000. **19**(5): p. 389-94.
70. Littlewood, T.D., et al., *A modified oestrogen receptor ligand-binding domain as an improved switch for the regulation of heterologous proteins*. Nucleic Acids Res, 1995. **23**(10): p. 1686-90.
71. Raetz, E.A., et al., *The nucleophosmin-anaplastic lymphoma kinase fusion protein induces c-Myc expression in pediatric anaplastic large cell lymphomas*. Am J Pathol, 2002. **161**(3): p. 875-83.

72. Breit, S. and M. Schwab, *Suppression of MYC by high expression of NMYC in human neuroblastoma cells*. J Neurosci Res, 1989. **24**(1): p. 21-8.
73. Westermann, F., et al., *Distinct transcriptional MYCN/c-MYC activities are associated with spontaneous regression or malignant progression in neuroblastomas*. Genome Biol, 2008. **9**(10): p. R150.
74. Schonherr, C., et al., *Anaplastic Lymphoma Kinase (ALK) regulates initiation of transcription of MYCN in neuroblastoma cells*. Oncogene, 2012.
75. Berry, T., et al., *The ALK(F1174L) mutation potentiates the oncogenic activity of MYCN in neuroblastoma*. Cancer Cell, 2012. **22**(1): p. 117-30.
76. Lemmon, M.A. and J. Schlessinger, *Cell signaling by receptor tyrosine kinases*. Cell, 2010. **141**(7): p. 1117-34.
77. Xu, A.M. and P.H. Huang, *Receptor tyrosine kinase coactivation networks in cancer*. Cancer Res, 2010. **70**(10): p. 3857-60.
78. Schonherr, C., et al., *Activating ALK mutations found in neuroblastoma are inhibited by Crizotinib and NVP-TAE684*. Biochem J, 2011. **440**(3): p. 405-13.
79. Schulte, J.H., et al., *The low-affinity neurotrophin receptor, p75, is upregulated in ganglioneuroblastoma/ganglioneuroma and reduces tumorigenicity of neuroblastoma cells in vivo*. Int J Cancer, 2009. **124**(10): p. 2488-94.
80. Vitali, R., et al., *Slug (SNAIL2) down-regulation by RNA interference facilitates apoptosis and inhibits invasive growth in neuroblastoma preclinical models*. Clin Cancer Res, 2008. **14**(14): p. 4622-30.
81. Isogai, E., et al., *Oncogenic LMO3 collaborates with HEN2 to enhance neuroblastoma cell growth through transactivation of Mash1*. PLoS ONE, 2011. **6**(5): p. e19297.
82. Reiff, T., et al., *Neuroblastoma phox2b variants stimulate proliferation and dedifferentiation of immature sympathetic neurons*. J Neurosci, 2010. **30**(3): p. 905-15.
83. Bielle, F., et al., *PHOX2B immunolabeling: a novel tool for the diagnosis of undifferentiated neuroblastomas among childhood small round blue-cell tumors*. Am J Surg Pathol, 2012. **36**(8): p. 1141-9.
84. Munchar, M.J., et al., *CD44s expression correlated with the International Neuroblastoma Pathology Classification (Shimada system) for neuroblastic tumours*. Pathology, 2003. **35**(2): p. 125-129.
85. Valentiner, U., F.U. Valentiner, and U. Schumacher, *Expression of CD44 is associated with a metastatic pattern of human neuroblastoma cells in a SCID mouse xenograft model*. Tumour Biol, 2008. **29**(3): p. 152-60.
86. Zhang, H., et al., *Biomimetic three-dimensional microenvironment for controlling stem cell fate*. Interface Focus, 2011. **1**(5): p. 792-803.
87. Bissell, M.J. and M.A. Labarge, *Context, tissue plasticity, and cancer: are tumor stem cells also regulated by the microenvironment?* Cancer Cell, 2005. **7**(1): p. 17-23.
88. Knudson, A.G., Jr., *Introduction to the genetics of primary renal tumors in children*. Med Pediatr Oncol, 1993. **21**(3): p. 193-8.

CURRICULUM VITAE

Personal informations

First names : Gisèle, Salomé
 Last name : Montavon
 Date of birth : 23.11.1986
 Place of birth : Yverdon-les-Bains, Switzerland
 Address : Pérolles d'en Haut 9
 1752 Villars-sur-Glâne, Switzerland
 Tel : 0041 79 300 07 39
 Mail : gi.montavon@gmail.com

Education

12.2011-11.2012	MD project entitled "Role of ALK gene in initiation and progression of neuroblastoma", Group of Dr. Nicole Gross, Paediatric Oncology Research Unit, Department of Paediatrics, University Hospital (CHUV), University of Lausanne, Switzerland
11.2011	Diploma of medicine, Swiss Confederation
2008-2011	Master in medicine, University of Lausanne, Switzerland
2005-2008	Bachelor in medicine, University of Lausanne, Switzerland
2002-2005	Swiss Baccalauréat, i.e. High School Leaving Diploma, Yverdon, Switzerland

Residency in medicine

11.2013-current	Paediatrics, Hospital of Fribourg, Switzerland
12.2012-10.2013	Internal medicine, Hospital of Yverdon, Switzerland

Internship in medicine

03.2011	General medicine, Office of Drs Zufferey-Andermatten, Vissoie, Switzerland
12.2010-02.2011	Paediatrics, University Hospital of Lausanne (CHUV), Switzerland
09.2010-10.2010	Infectious and tropical diseases, St-Louis Hospital, Paris, France
07.2010	Surgery, Hospital of Sion, Switzerland
05.2010-06.2010	Internal medicine, Hospital of Yverdon, Switzerland

Written works

- 2012-2013 Doctorate in Medicine entitled “Role of *ALK* gene in initiation and progression of neuroblastoma”, Group of Dr. Nicole Gross, Paediatric Oncology Research Unit, Department of Paediatrics, University Hospital (CHUV), University of Lausanne, Switzerland
- 2010 Master’s work entitled “Diagnostic prénatal du neuroblastome stade 4S agressif”, University of Lausanne, Switzerland
- 2004 Baccalaureate’s work entitled “Pluralisme culturel et social dans le monde de la santé”, High School of Yverdon, Switzerland

Publications

- 10.2012 Abstract entitled "Prenatal diagnosis of aggressive stage 4S neuroblastoma", Pediatric Blood & Cancer, in context of the SIOP (International Society of Paediatric Oncology)’s Congress in London

Scientific skills

- Molecular biology* RNA extractions from cultured cells and frozen tissues, protein extraction from cultured cells, cDNA synthesis, reverse-transcriptase PCR, real-time PCR, Western-Blot, retroviral-mediated infection
- Cell biology* Cell line culture, flow cytometry and cell sorting, cell viability assay, methylcellulose assay, sphere assay, cell differentiation assay
- In vivo experiment* Sub-cutaneous injection in mouse model, sub-cutaneous and orthotopic tumour resection, preparation of paraffin-embedded sections
- Microscopy* Analysis of H&E and IHC
- Computer skills* Microsoft Office (Word, Excel, Power-Point), Adobe Photoshop, GraphPad Prism, EndNote X5

Languages

- French Native
- English Relatively fluent
- German Baccalaureate level